

University of Mississippi

eGrove

Honors Theses


Honors College (Sally McDonnell Barksdale
Honors College)

Spring 5-1-2021

A Conductivity Analysis of a Newly Synthesized Poly(Ethylene Glycol) Methyl Ether Hydroxide Electrolyte

Sarah Marie Peterson
University of Mississippi

Follow this and additional works at: https://egrove.olemiss.edu/hon_thesis

 Part of the [Analytical Chemistry Commons](#), [Inorganic Chemistry Commons](#), [Oil, Gas, and Energy Commons](#), [Other Chemistry Commons](#), and the [Polymer Chemistry Commons](#)

Recommended Citation

Peterson, Sarah Marie, "A Conductivity Analysis of a Newly Synthesized Poly(Ethylene Glycol) Methyl Ether Hydroxide Electrolyte" (2021). *Honors Theses*. 1798.
https://egrove.olemiss.edu/hon_thesis/1798

This Undergraduate Thesis is brought to you for free and open access by the Honors College (Sally McDonnell Barksdale Honors College) at eGrove. It has been accepted for inclusion in Honors Theses by an authorized administrator of eGrove. For more information, please contact egrove@olemiss.edu.

A CONDUCTIVITY ANALYSIS OF A NEWLY SYNTHESIZED POLY
(ETHYLENE GLYCOL) METHYL ETHER HYDROXIDE ELECTROLYTE

by
Sarah Peterson

A thesis submitted to the faculty of the University of Mississippi in partial
fulfillment of the requirements of the Sally McDonnell Barksdale Honors College

Oxford
April 2021

Approved by:

Advisor: Dr. Jason Ritchie

Reader: Dr. Nathan Hammer

Reader: Dr. Kerri Scott

© 2021
Sarah Peterson
ALL RIGHTS RESERVED

DEDICATION

I would like to dedicate my thesis first to my parents, Laura and Jeff Peterson, because without their support I would have never chosen Ole Miss to spend these past four years. Their unwavering faith in my abilities has encouraged me every day. I would also like to dedicate this to my friends and all past roommates who listened to me explain complex chemistry theory and just nodded their heads. Finally, I would like to dedicate this thesis to Olivia Fox and all future undergraduate students in Dr. Ritchie's Lab who experience the same technological hardships in conductivity analysis and polymer synthesis.

ACKNOWLEDGEMENTS

I would like to thank Dr. Jason Ritchie for allowing me to research in his lab these past four years. He was an incredible mentor and support system for myself and other students in the lab and always offered kind and instructive words. This project would not have been possible without his immense patience. I would also like to thank the Sally McDonnell Barksdale Honors College for guiding me throughout these past four years. The opportunities for growth as a student and an individual have been invaluable and I will be forever grateful for this program. I finally want to thank my academic advisor, Dr. Nathan Hammer, who has helped me through every trial I faced as a student and offered great advice over the course of undergraduate studies.

ABSTRACT

This thesis investigates the synthesis and conductive properties of a Poly (ethylene glycol) methyl ether-based polymer electrolyte. The goal of the synthesis is to enhance the hydroxide ion conduction properties of the polymer with its cationic groups attached. The MePEG backbone contained seven ethylene glycol groups and was modified to substitute the hydroxide group in the MePEG with trimethylamine. In addition, the bromide added in the synthesis was exchanged for hydroxide ions to allow for the transportation of hydroxide ions in polymeric electrolytes that can be used in Anion Exchange Membrane Fuel Cells. The newly synthesized polymer was compared to the backbone of the polymer, MePEG₇, using lithium ions to measure the conductivity. The conductive analysis in anhydrous environments yielded a temperature based ionic conductivity study and the activation energy that is needed to transport the ions across the membrane. This analysis helped to characterize the potential viability of the MePEG based polymeric electrolytes in anion exchange membranes based on its conductivity and activation energy.

TABLE OF CONTENTS

DEDICATION	iii
ACKNOWLEDGEMENTS	iv
ABSTRACT	v
LIST OF ABBREVIATIONS	vii
LIST OF FIGURES	ix
INTRODUCTION	1
EXPERIMENTAL	15
Synthesis of MePEG ₇ Br	15
Synthesis of MePEG ₇ NMe ₃ ⁺ Br ⁻	20
Ion Exchange of MePEG ₇ NMe ₃ ⁺ Br ⁻ to MePEG ₇ NMe ₃ ⁺ OH ⁻	23
Formation of MePEG ₇ Li ⁺ Solution	25
Conductivity Measurements	26
Sample Calculations to Determine E _a from Nyquist Plot	31
Molar Conductivity Measurements	31
RESULTS AND DISCUSSION	32
AC Impedance Dummy Cell 1700-1126-REV	32
Conductivity Results	33
CONCLUSION	42
REFERENCES	45

LIST OF ABBREVIATIONS

E₀	Standard Cell Potential (V)
V	Voltage
H	Efficiency (V)
AFC	Alkaline Fuel Cell
AEMFC	Anion Exchange Membrane Fuel Cell
DMFC	Direct Methanol Fuel Cell
PEMFC	Proton Exchange Membrane Fuel cell
CHP	Combined Heat and Power
PEM	Proton Exchange Membrane
ORR	Oxygen Reduction Reaction
AEM	Anion Exchange Membrane
OH⁻	Hydroxide Ion
MePEG	Poly (ethylene glycol) methyl ester
MePEG₇	Poly (ethylene glycol) methyl ester MW = 350
NMe₃	trimethylamine
S	Siemens
Z	Impedance
R	Resistance
AC	Alternating Current
DC	Direct Current
ρ	Resistivity (Ω/cm)
l/A	Cell Constant (cm ⁻¹)

NMR	Nuclear Magnetic Resonance
CDCl₃	Deuterated Chloroform
DCM	Dichloromethane
K	Kelvin
kJ	kilo Joules
Ω	Ohm
σ	Conductivity (S/cm)
E_a	Activation Energy (kJ/mole)
Λ	Molar Conductivity (S cm ² mole ⁻¹)

LIST OF FIGURES

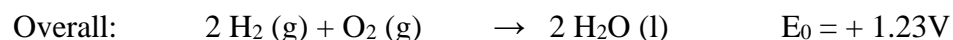
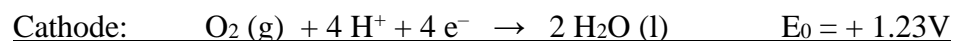
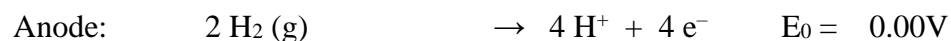
Figure 1	Cross Section of a Fuel Cell. Figure adapted from Reference ¹	3
Figure 2	Anion Exchange Membrane Fuel Cell (AEMFC). Figure adapted from Reference ¹⁵	8
Figure 3	Factors to consider for the development of AEMs. Figure adapted from Reference ²⁰	9
Figure 4	General Structure of Poly (ethylene glycol) Methyl Ether. Figure adapted from Reference ¹³	10
Figure 5	Nyquist Plot. Figure adapted from Reference ¹⁰	11
Figure 6	Synthesis of MePEG ₇ Br (MW = 412.904 g/mol)	16
Figure 7	¹ H NMR for MePEG ₇ OH reactant (top) and MePEG ₇ Br product (bottom)	18
Figure 8	¹³ C NMR for MePEG ₇ OH reactant (top) and MePEG ₇ Br product (bottom)	19
Figure 9	Synthesis of MePEG ₇ NMe ₃ ⁺ Br ⁻ (MW = 472.015 g/mol)	20
Figure 10	The ¹ H NMR for MePEG ₇ NMe ₃ ⁺ Br ⁻	21
Figure 11	The ¹³ C NMR for MePEG ₇ NMe ₃ ⁺ Br ⁻	22
Figure 12	Synthesis of MePEG ₇ NMe ₃ ⁺ OH ⁻ (MW = 409.11 g/mol)	23
Figure 13	The ¹ H NMR for MePEG ₇ NMe ₃ ⁺ CH ₃ SO ₃ ⁻	24
Figure 14	The ¹³ C NMR for MePEG ₇ NMe ₃ ⁺ CH ₃ SO ₃ ⁻	25
Figure 15	Perkin-Elmer 5210 Lock-in Amplifier (top) and PAR 283 Potentiostat (bottom)	26

Figure 16	A Faraday Cage (left) Enclosing the Temperature and Vacuum Controlled Electrode System (right)	27
Figure 17	MaximaDry Vacuum Pump (left) and an Isotemp 3016 Water Heater and Cooler (right)	28
Figure 18	AC Impedance Dummy Cell 1700-1126-REV. 0	29
Figure 19	The Parameters for the Conductivity Measurements in PowerSuite	30
Figure 20	Nyquist Plot for AC Impedance Dummy Cell which had a diameter of 99.81 Ω	33
Figure 21	Nyquist Plot of MePEG ₇ Li ⁺ at 20 °C which had a diameter of 450,400 Ω and conductivity of 2.22*10 ⁻⁶ S/cm	34
Figure 22	Nyquist Plot of MePEG ₇ NMe ₃ ⁺ OH ⁻ at 20 °C which had a diameter of 433,500 Ω and conductivity of 2.31*10 ⁻⁶ S/cm	35
Figure 23	Temperature dependent conductivity measurements for MePEG ₇ Li ⁺ and MePEG ₇ NMe ₃ ⁺ OH ⁻	36
Figure 24	Temperature dependent molar conductivity measurements for MePEG ₇ Li ⁺ and MePEG ₇ NMe ₃ ⁺ OH ⁻	37
Figure 25	Arrhenius Activation Plot for MePEG ₇ Li ⁺ , best fit line and coefficient of determination displayed.	38
Figure 26	Arrhenius Activation Plot for MePEG ₇ NMe ₃ ⁺ OH ⁻ , best fit line and coefficient of determination displayed.	41

INTRODUCTION

Fuel cells are devices that generate electricity through an electrochemical reaction. Much of the energy used in everyday life is powered by combustion reactions which release carbon emissions and other potential toxic waste.⁵ Fuel cells are an alternative fuel source that are clean, reliable, efficient, and a quiet source of power. They are becoming increasingly common and have a wide variety of uses. Their application ranges from powering cars to laptops, to providing power to business and critical facilities such as hospitals.⁵ The need for clean, renewable, and efficient energy sources is growing. The depletion of nonrenewable energy sources such as coal, natural gases, and petroleum along with the concern over the rising carbon emission levels demands other forms of energy quickly. Fuel cell reactions, which produce no pollutants, carbon emissions, and are sources for renewable energy, may be the answer to this problem.⁴

Fuel cells are comprised of a cathode, anode, and an electrolyte membrane and work much like a battery. In the Polymer Electrolyte Membrane Fuel Cell (PEMFC), Hydrogen gas is passed through the anode of the fuel cell and oxygen gas through the cathode which results in the production of water and electricity.⁴



In this reaction, the hydrogen is being oxidized at the anode, losing electrons which then move through the external circuit as electricity. The hydrogen ions (H^+) are then able to move through the electrolyte membrane to the cathode portion of the cell where they combine with the oxygen gas, and electrons returning from the electrical circuit to produce water at the cathode.³

The reaction occurring in fuel cells can be broken down into four different steps as shown in *Figure 1*: (1) reactant delivery into the fuel cell, (2) electrochemical reaction, (3) ionic conduction through the electrolyte and electronic conduction through the external circuit, and (4) product removal from fuel cell.¹ It is important for the fuel and oxidant, hydrogen gas and oxygen gas, respectively in a PEM fuel cell, to be constantly supplied so the device doesn't starve and stop the production of electricity. The electrochemical reaction can then constantly occur. The fuel needs to be oxidized at the anode so it can release electrons to the circuit. An electrocatalyst is needed to help this reaction occur quickly. Typically, Platinum metal is used as the electrocatalyst for the Hydrogen Oxidation Reaction (HOR).

Since the ions produced in the electrochemical reaction are produced at the anode, and then consumed at the cathode, an electrolyte is required in order to provide a pathway for them to cross the cell. The diffusion of the H^+ ions is a much less efficient process than the conduction of electrons through an external electrical circuit. The anode and cathode reactions provide an electromotive force for the overall chemical reaction, and thus there is a voltage difference between the anode and cathode which can be used to do

electrical work in the external circuit. The overall cell potential can be calculated from the following equation:

$$E^0_{\text{cell}} = E^0_{\text{reduction (cathode)}} - E^0_{\text{reduction (anode)}}$$

In the PEM fuel cell, the E^0 of the cathode is +1.23V and the E^0 of the anode is 0.00V, which makes the overall $E^0_{\text{cell}} = + 1.23\text{V}$. Typically, many cells would be stacked together, and connected in series in order to generate a higher DC output voltage, which could be used to drive an electric motor of a car, or just serve as a stationary power source.

Once at the cathode, the oxidant, electrons, and ions combine to form water as the only product of the reaction, which, depending on the operating temperature, can then exit the fuel cell.¹

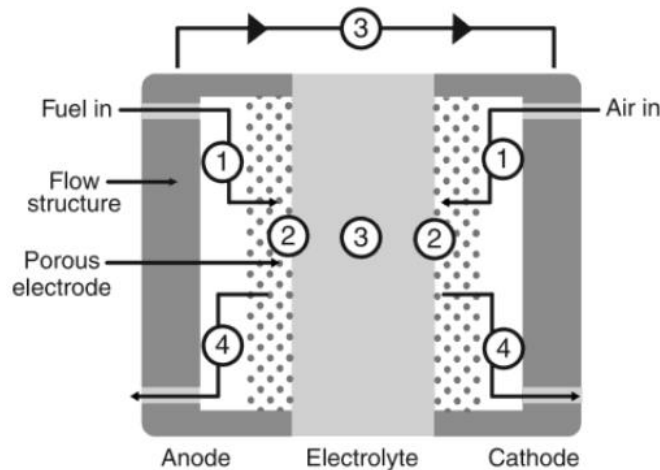


Figure 1: Cross Section of a Fuel Cell. The fuel enters the cell at (1) and undergoes an electrochemical reaction (2). The ions produced in the reaction cross the electrolyte (3) and the electrons flow through the circuit (3). The product is produced and exits the system (4). Figure adapted from Reference.¹

The electric current produced by the electrons flowing from the anode to cathode is directly proportional to the amount (moles) of fuel consumed. Since voltage and current have a direct relationship as stated by Ohm's Law, the electric power produced per unit of fuel increases or decreases according to the fuel cell voltage. Maintaining high levels of voltage is crucial for the success of this technology. However, this is hard to maintain and results in a difference between the predicted voltage (E_{thermo}) and the real voltage produced (V).¹ There are three factors that contribute to the loss of voltage in a fuel cell: activation loss (η_{act}), ohmic loss (η_{ohmic}), and concentration loss (η_{conc}).¹ The activation loss occurs from the electrochemical reaction. The ohmic loss is caused by the ionic and electronic conduction; however, the ionic loss contributes significantly more because ions are larger and harder to transport. The concentration loss is due to mass transport. As the amount of current flowing through the fuel cell increases, these losses also increase, causing the fuel cell to become more inefficient at larger scales.¹

$$V = E_{\text{thermo}} - \eta_{\text{act}} - \eta_{\text{ohmic}} - \eta_{\text{conc}}$$

There are several major types of fuel cells which differentiate mostly by the type of electrolyte used to allow the ions to flow through, however, only the only four that will be focused on are Alkaline (AFC), Anion Exchange Membrane (AEMFC), Direct Methanol (DMFC), and Proton Exchange Membrane (PEMFC).² AFC is unique in that it moves hydroxide ions across the electrolyte membrane which is comprised of a liquid electrolyte such as potassium hydroxide, KOH. The platinum cathode electrocatalyst in an AFC is very efficient, which when combined with highly porous electrodes help overcome the problem of slow reaction rates in this cell. This is a major efficiency

advantage for this type of cell, as most other types of cells lose a lot of voltage in their Oxygen Reduction Reaction (ORR) electrode. In addition, these cells are typically operated at high pressures and lower temperatures. Its range is 50-200 °C, however, they typically operate less than 100 °C. The biggest challenge with this fuel cell is that any carbon dioxide present in the oxidant or fuel streams will dissolve in the alkaline electrolyte and be precipitated as a carbonate salt. Thus, the air and fuel supplies of an AFC must be completely free of CO₂. AFCs have been used in several NASA space craft, such as the Apollo and STS Shuttle vehicles, where they typically have pure oxygen available.²

Polymer Electrolyte Membrane Fuel Cells and Direct Methanol Fuel Cells are potentially applicable for automotive and small to medium scale stationary use and are some of the most promising alternative energy conversion devices for consumer use. PEMFCs are used in current fuel cell powered vehicles and for mobile applications as well as low-power combined heat and power systems (CHP), which are systems that generate electricity and capture heat that would otherwise be wasted to provide heat for multiple different facilities.⁸

PEMFCs and DMFCs both contain an immobile electrolytic polymer membrane that allows a H⁺ ion to pass through and operate at temps between 30-100 °C. Due to slow reaction kinetics, a platinum catalyst is required. This is a major disadvantage, as the platinum is very expensive. Finding alternative, more earth-abundant electrocatalyst materials would be required for large scale deployment of this technology. In addition, because of the platinum electrodes, these cells need mostly pure hydrogen gas that is free of Carbon monoxide. Hydrogen is not a fossil fuel, but it is produced as an energy storage

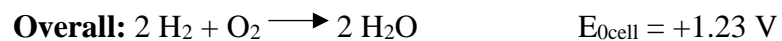
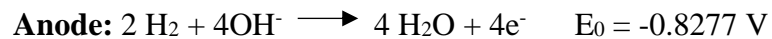
material. Most hydrogen is produced by the steam reformation of natural gas and coal, which produces CO as an intermediate that can contaminate the product hydrogen gas stream.

DMFCs attempt to solve this problem by using methanol as fuel instead of hydrogen gas.² The methanol can be used in the PEM cell meaning it operates at similar temperatures and uses the same catalyst and electrolyte to move protons. These cells can be used in portable electronic systems that run at low power for long times. The most expensive part of either of these two methods is the platinum catalyst, however, less and less platinum has been needed over the years due to developments. DMFCs have the advantage of using a liquid fuel, which is much easier to refuel and store compared to a high-pressure gas like H₂, and can use air as the oxidant stream. However, DMFCs have substantial challenges associated with electroosmotic crossover of the methanol fuel from the anode to the cathode.

PEM fuel cells are the focus of a fair amount of fuel cell research due to their attractiveness for many different applications caused by the cells ability to operate at low temperatures with high power density.² The different areas of research for the PEM and fuel cells can range from the fuel used to the electrolyte material. Since platinum is a very expensive catalyst, substitutes for it are sought after or methods to reduce the quantity of platinum needed for the cell to run adequately.⁶ In addition, the cell's fuel is another source of development. Since pure hydrogen sources can be problematic because it can be expensive. Methanol would be a good substitute because it is a cheaper source of fuel, however, the low power production poses a problem. Another major source of research is the polymer electrolyte.⁶ The goal from this research is to increase the mobility of the

protons, create electrolytes that can operate at higher temperatures, and to increase the degree of ionic conductivity of the electrolyte.

AEMFCs, also called Alkaline Anion Exchange fuel cells (AAEFCs), are less researched than the PEMFCs even though they work with the same parameters. PEMFCs transport H^+ ions across the polymer electrolyte while AEMFCs transport hydroxide (OH^-) ions across the polymer electrolyte. AEMFCs have several advantages over their PEMFC counterparts. The basic oxygen reduction reaction (ORR) that combines the electrons with the O_2 gas occurs much easier in alkaline solutions than acidic solutions which could potentially allow for less expensive catalysts to be used.⁷ PEMFCs experience a degradation in polymer thickness because of the of dehydration of the polymer electrolyte. This is accelerated when the fuels, typically H_2 and Methanol, crossover. The electroosmotic drag opposes the crossover of liquid fuel in AEMFCs which permits more concentrated fuels which is an advantage for portable applications.⁷ The improved kinetics with the cathode reaction and the opposition of crossover allows for more flexibility regarding the catalyst needed are just some of the reasons why AEMFCs are attractive for the future of ion exchange membranes.



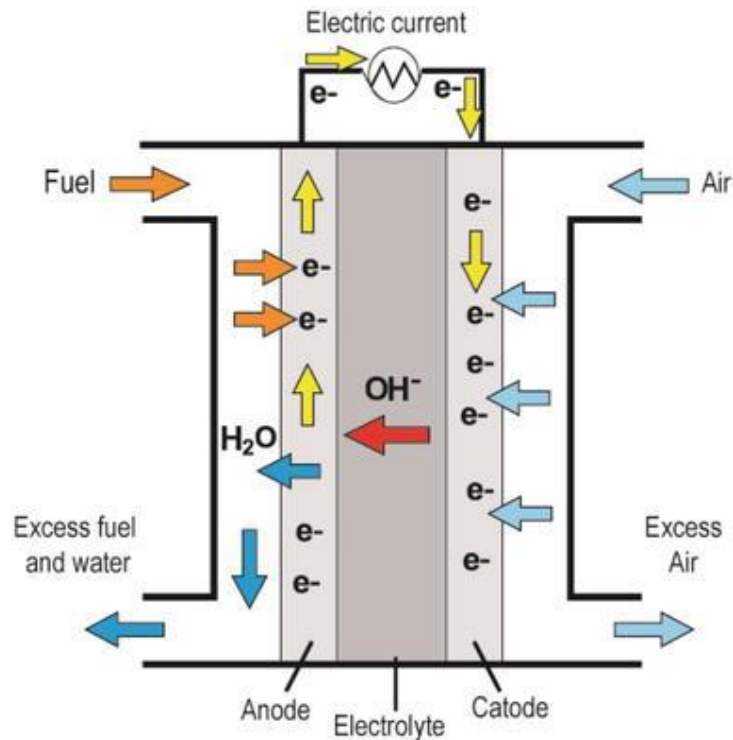


Figure 2: Anion Exchange Membrane Fuel Cell (AEMFC). Figure adapted from Reference¹⁵

In the current research stages of the anion exchange membranes (AEMs), the polymers have a fixed cationic group to keep the molecule immobile in the liquid electrolyte.¹¹ This is to prevent the formation of carbonate precipitates that stem from the carbon dioxide in the air. However, at the site where the cationic group is added, there can be poor chemical stability. This, along with the low ionic conductivity of AEMs and poor solubility in inexpensive solvents are the reason that these fuel cells are not as popular as PEMFCs. The challenge in making AEMs with high OH^- conductivity is to ensure that it also has good mechanical properties. The addition of cationic sites can increase the ionic conductivity; however, this could also cause excessive swelling when fully hydrated and brittleness when the molecule is partially or completely dry.¹¹ There

are a multitude of other parameters to consider for the research and development of AEMs which can be seen in *Figure 3*.

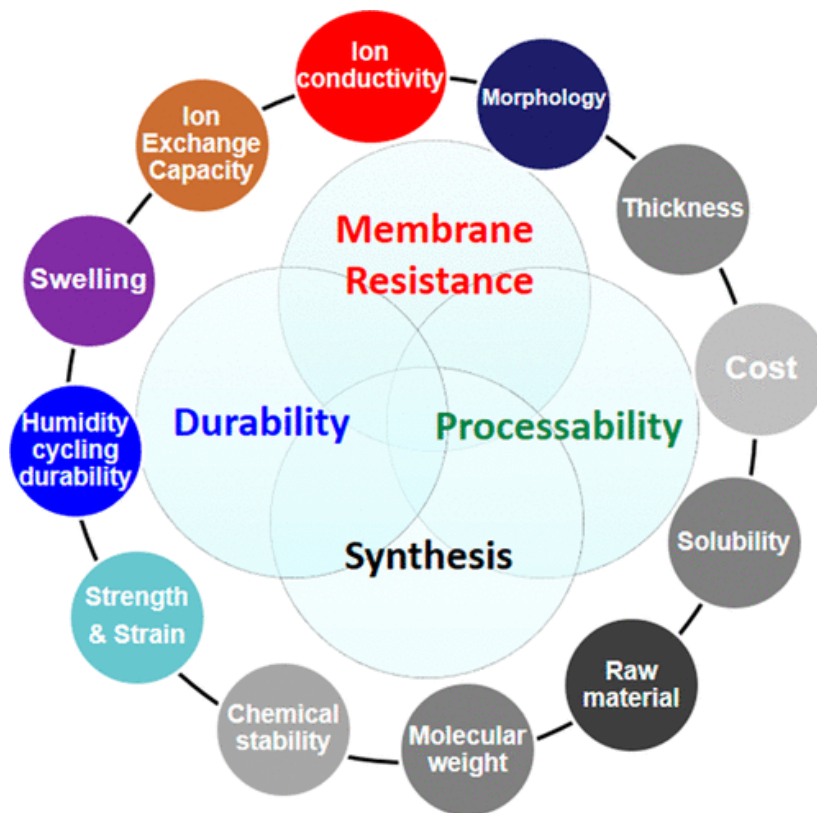


Figure 3: Factors to consider for the development of AEMs. Figure adapted from Reference²⁰

Poly (ethylene glycol) methyl ether (MePEG), shown in *Figure 4*, can be used as the polymer backbone in AEM or PEM. These are hydrophilic, water soluble molecules that can be used to create very high osmotic pressures.¹² These properties make it useful as a polymer membrane in a fuel cell that undergoes ORR to produce water. In addition, these molecules can have cationic groups added to them to allow for OH⁻ ions to pass through the membranes. In this project, the cationic structure added to the MePEG was

trimethylamine (NMe₃). Our research group has previously made a similar molecule with an imidazolium based cationic group.¹⁹

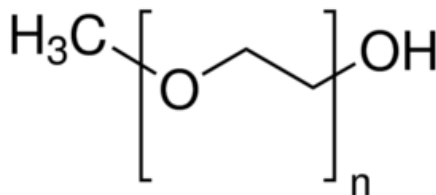


Figure 4: General Structure of Poly (ethylene glycol) Methyl Ether. Figure adapted from Reference¹³

Ionic Conductivity measurements are used to determine the ionic conductivity in the anion or proton exchange membrane. It is the measure of the materials ability to allow ions to diffuse through it and conductivity is measured in Siemens/cm.⁹ To obtain the conductivity value of a molecule, the impedance must be measured. Impedance is the measure of the ability of a circuit to resist the flow of an electrical current that is not limited to simplifying properties associated with idealistic resistors. This measurement is capable of measuring the complexities that exist in real world complex behavior. The impedance is represented as a complex number shown below.⁹

$$Z(\omega) = \frac{E}{I} = Z_0 \exp(j\Phi) = Z_0(\cos\Phi + j\sin\Phi)$$

The impedance can be identified using a Nyquist plot as shown in **Figure 5** which displays Z_ω in both a real, Z_{re} , (x-axis, resistance) and imaginary, $-Z_i$, (y-axis, capacitance) components.¹⁰ A limitation of the Nyquist plot is that it doesn't display the frequency associated with each point. However, the R_{AB} , or the diameter of the circle, is

the bulk ionic resistance of the substance being measured. The R_{BC} displays a tail which is known as a Warburg effect. The effect occurs due to diffusion and occurs at lower frequencies when reactants have to diffuse further. The Warburg tails almost seem to exhibit DC impedance if the frequency range is low enough.⁹

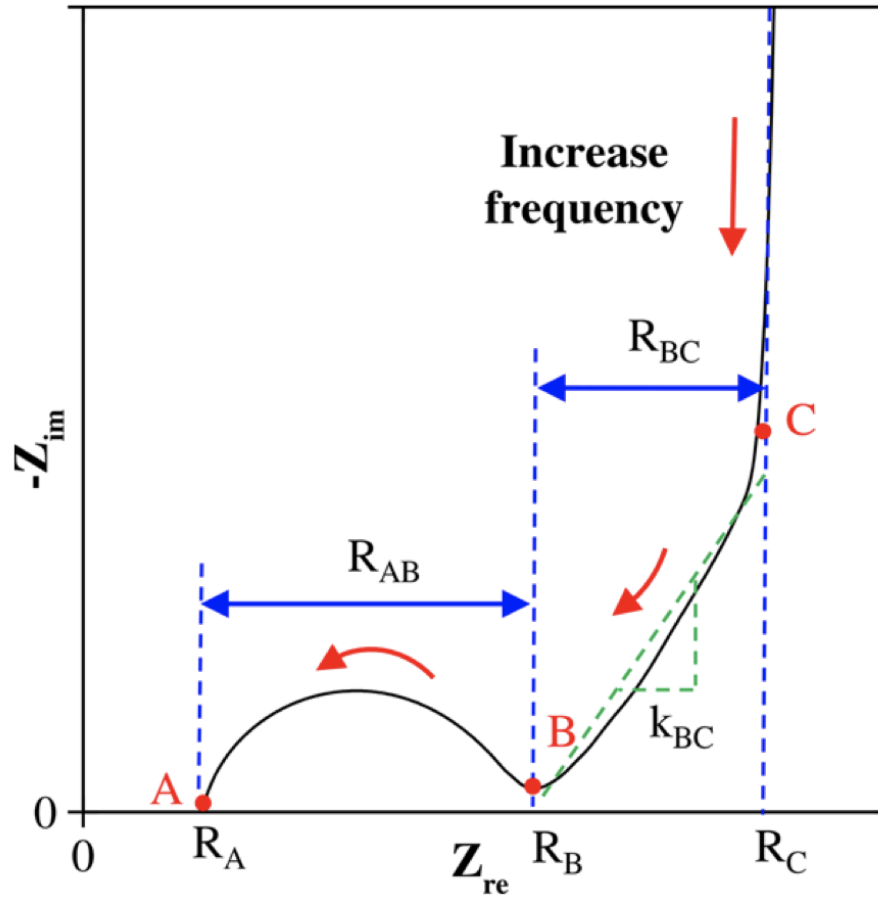


Figure 5: Nyquist Plot. Figure adapted from Reference¹⁰

The resistance of the electrolyte solution depends on the ionic concentration, types of ions, temperature, and geometry of the area in which the current is carried. The resistance is measured between the working and reference electrode in the cell and is

defined in the equation below that compares resistance, R , to the solutions resistivity, ρ , and the geometry (length, l , and area, A) of the cell electrodes.⁹

$$R = \rho \frac{l}{A}$$

The reciprocal of resistivity is conductivity, σ , which is a more commonly used method of presenting the results of this measurement. Conductivity can therefore be thought of as the conductance multiplied by the cell constant (l/A) of the conductivity electrode. The conductivity of the synthesized polymer in this paper was measured using an AC-impedance spectroscopy using an Electrochemical Potentiostat (PAR Model 283) and a Perkin-Elmer 5210 lock-in amplifier.

The polymer's ionic conductivity is a function of several different factors. The first of which is temperature: The kinetics of ion transport in the solution are affected by the temperature which is reflected in the measured ionic conductivity. As temperature increases, the kinetic energy of the diffusing molecules and electrode reaction rates increase, which decreases the resistance of the electrolyte. because the redox reaction is shifted towards the products. Another factor that affects the conductivity of the solution is the presence of water in the air during the measurements. Water acts as a "plasticizer" in our polymer electrolyte, and increases the rate of polymer reorganization, which leads to faster diffusion. Thus, when water is introduced to the polymer electrolyte, the ionic conductivity increases. This is normal for AEMFCs, and a lot of effort is devoted to trying to manage the water in the fuel cell electrolyte, and to keep it from losing all the water at higher temperatures. In our experiments, we are specifically interested in understanding the ability of our polymer electrolyte to be able to conduct OH^- ions under

high temperature conditions that rapidly vaporize water from the fuel cell electrolyte. In addition, testing our polymer electrolyte samples under “wet” conditions leads to rapidly increased conductivity values which fall outside of the frequency range that our electrode and Potentiostat can measure.

In the literature, one way the conductivity of different ions and molecules can be compared is through the activation energy of ionic conductivity obtained from Arrhenius Activation plots. These plots describe the relationship between a rate constant, k , and the temperature, in Kelvin. By taking the natural log of the rate constant and the inverse of temperature, the linear slope yields the activation energy. The activation energy describes the minimum amount of energy needed for the chemical reaction to occur. In this project, instead of measuring a rate constant, the ionic conductivity is plotted instead. The ionic conductivity can be thought of as a rate in this system. The fuel is constantly being added to the system meaning a constant stream of ions passes through the electrolyte at a given time, thus, creating a measurable rate constant through conductivity.

The slope of $\log(\sigma)$ versus $1000/T$ yields the activation energy for the ionic transport. In this measurement, the activation energy for ionic conductivity can shed some light on the mechanism of ionic conductivity. For instance, how are the ions actually coordinated in the polymer electrolyte, and how do they move between coordination sites? The larger the activation barrier that is required to activate ionic transportation, the more ineffective the electrolyte is for an AEM or PEM. The goal is then to synthesize a molecule that has a low activation energy for the ionic transport which would create a more optimal membrane in the AEMFC.

Another common measurement used to analyze the conductivity properties of different electrolytic polymers is via molar conductivity. The molar equivalent conductivity (Λ) allows for an easier comparison of the ionic mobility of solutions with different polymers or different concentrations. It gives a more practical analysis of ionic conductivity in the literature. It is easily calculated by dividing the measured conductivity (S/cm) by the ionic concentration (mol/cm³) with the unit Siemens cm² mol⁻¹.

$$\Lambda = \frac{\sigma}{c}$$

EXPERIMENTAL

Synthesis of MePEG₇Br

In an air-free round-bottom flask, 43 mL of 1.0 M tribromophosphine (MW = 270.69 g/mol, 43 mmol), PBr₃, in dichloromethane (CH₂Cl₂, MW = 84.93 g/mol), DCM, was slowly added to a solution containing 30.0 g of poly(ethylene glycol) monomethyl ether (MePEG₇OH, MW= 350 g/mol, 85.7 mmol) and 50 mL of dry diethyl ether (MW = 74.12 g/mol), (C₂H₅)₂O. This reaction was stirred overnight at room temperature. It was then poured over 100 g of ice and extracted with 100 mL of diethyl ether and two portions of 100 mL of DCM. The solution was then dried with sodium sulfate (Na₂SO₄, MW = 142.04 g/mol) and concentrated using rotary evaporation. MePEG₇Br (412.9 g/mol) was recovered as the product, and yielded 30 g (72.7 mmol, 85% yield).¹⁷ Alcohol groups are normally not good leaving groups for organic reactions, however, in the presence of PBr₃, an unpaired electron pair forms a bond with the phosphate atom which in turn releases a free bromide ion. The alcohol has been converted into a good leaving group which allows for the free bromide ion to bond to the molecule. The general reaction can be seen in *Figure 6*.

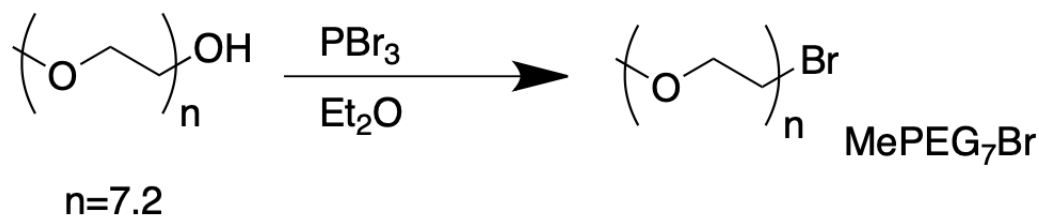


Figure 6: Synthesis of MePEG₇Br (MW = 412.904 g/mol)

To verify the success of the synthesis, Nuclear Magnetic Resonance (NMR) spectra were obtained for both ¹H, **Figure 7**, and ¹³C, **Figure 8**. The MePEG₇Br was analyzed in deuterated chloroform (CDCl₃ MW = 120.384 g/mol) for both spectra. In the proton spectrum, there are notable peaks at 3.38 ppm, 3.48 ppm, 3.66 ppm, and 3.81 ppm. As the reaction proceeds and the –CH₂OH group is converted into a –CH₂Br group, we expect the largest change in the NMR spectra to occur for those –CH₂– hydrogen adjacent to the alcohol/bromine atom. In this case, the signal seen at 3.60 ppm in the MePEG₇OH reactant completely disappears, and is replaced by a signal at 3.81 ppm in the MePEG₇Br product. These signals are likely these α–CH₂'s.

In the MePEG₇OH, the protons adjacent to the hydroxide group are more deshielded than its counterparts in the MePEG₇Br molecule.²¹ As the hydrogens get further away from the –CH₂Br group, we see less of an effect on their position in the spectra.

The ¹³C NMR displays similar patterns to the proton NMR. It has major peaks at 30.34 ppm, 59.01 ppm, 70.29-70.64 ppm, 71.19 ppm, 71.91 ppm, and 72.49 ppm. The peaks from 76.88-77.41 ppm represent the CDCl₃ and therefore are excluded from the data. The peak at 61 ppm most likely represents the carbon attached to the alcohol group in MePEG₇OH.²⁸ The peak at 30.34 ppm represents the carbon attached to the bromide

group in MePEG₇Br.²⁸ Notice the disappearance of the 61 ppm peak and the appearance of the 30 ppm peaks. This further verifies the proton NMR.

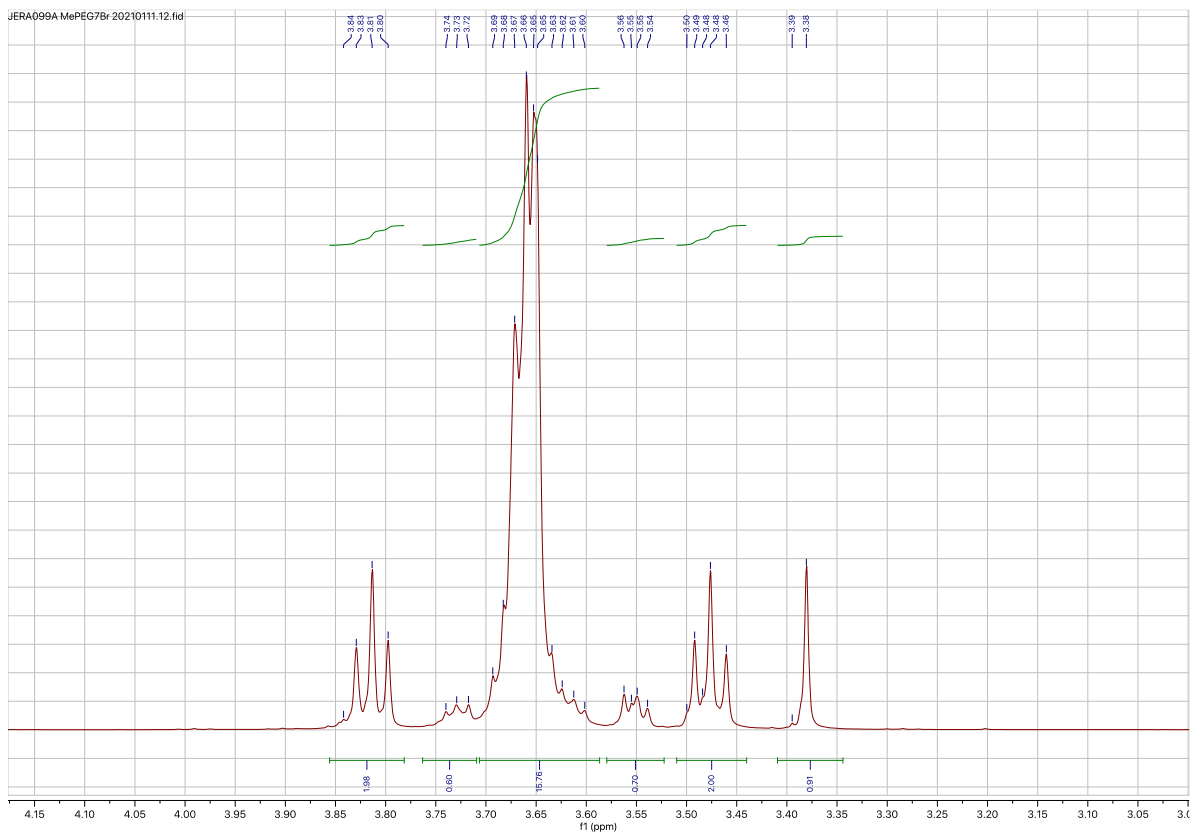
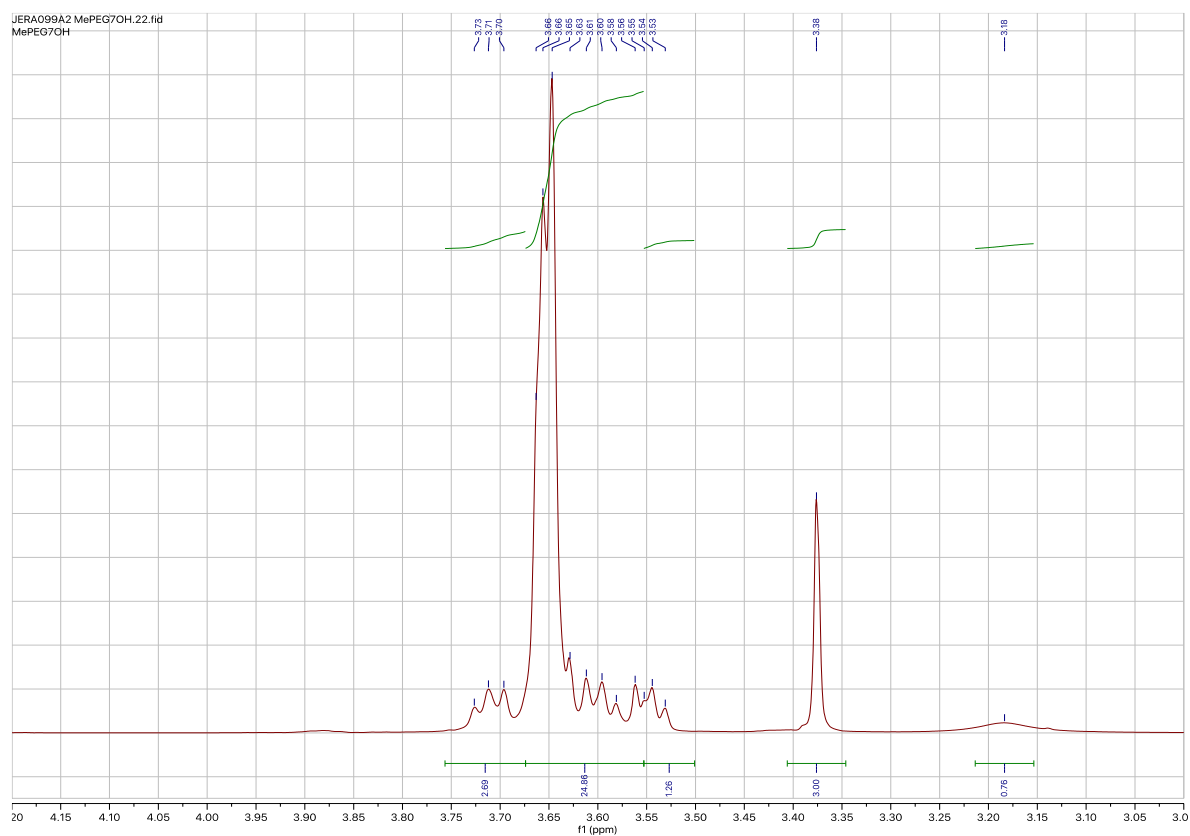


Figure 7: ^1H NMR for MePEG₇OH reactant (top) and MePEG₇Br product (bottom)

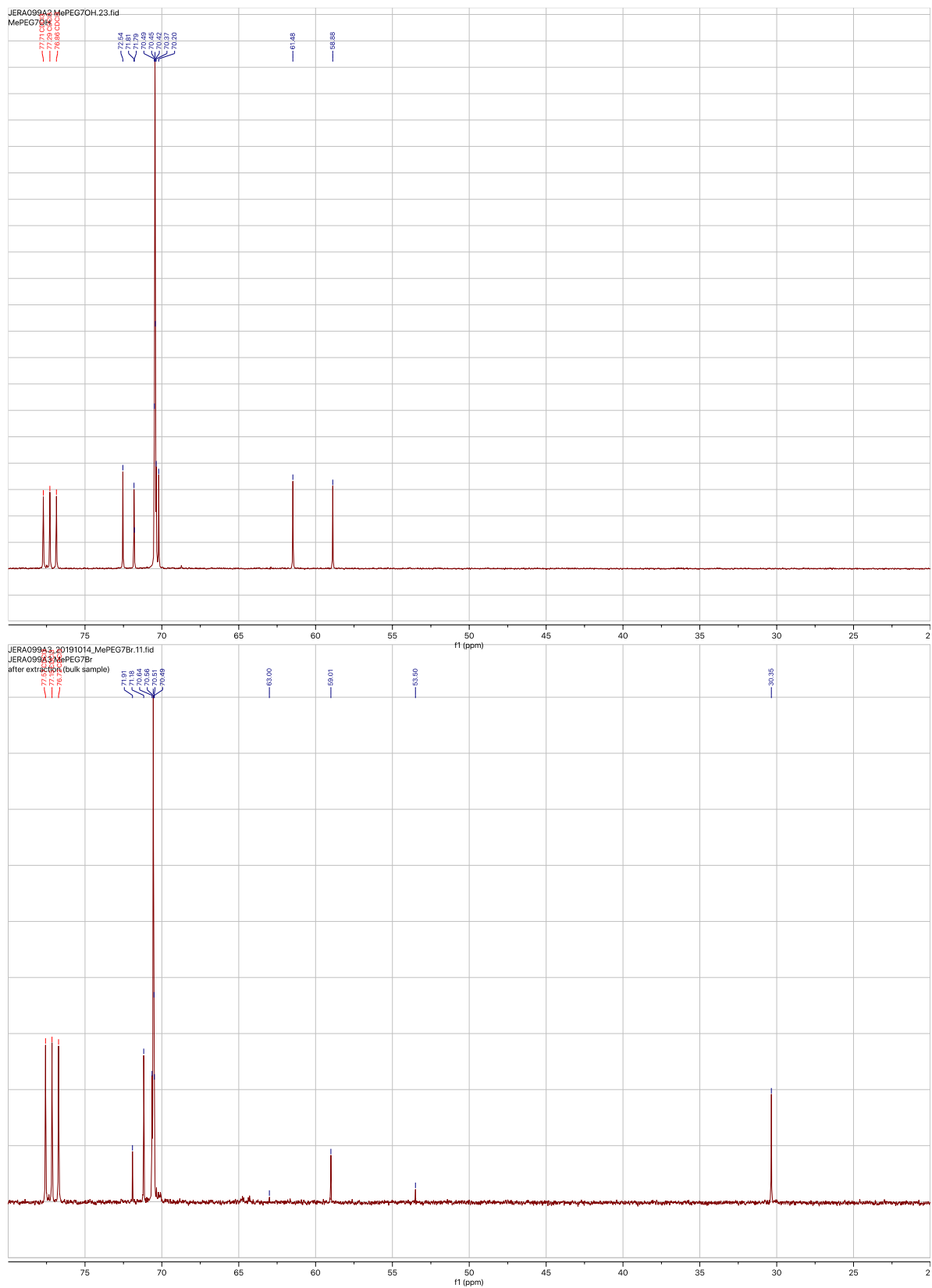


Figure 8: ^{13}C NMR for MePEG₇OH reactant (top) and MePEG₇Br product (bottom)

Synthesis of MePEG₇NMe₃⁺ Br⁻

In the synthesis of MePEG₇NMe₃⁺ Br⁻, the high electronegativity of the bromide allows it to act as a leaving group in the presence of water. The NMe₃ can then act as a nucleophile creating the product. The reaction can be seen in **Figure 9**. In a round-bottom flask, 5.41 mL of a 30% solution NMe₃ (33% by weight, 4.2M, MW = 59.11 g/mol, 22.7 mmol) in ethanol (C₂H₅OH, MW = 46.07 g/mol) was added dropwise to 1.53 g of MePEG₇Br (MW = 412.90 g/mol, 3.71 mmol) in an ice bath with a stir bar. The flask was immediately capped with a plastic pop-off cap. This is important because since this reaction took place at room temperature, the NMe₃ can be released as a gas and would escape if not sealed. In addition, if too much pressure is generated from this reaction, it is important for it to be released so the equipment does not explode. After 8 hours of stirring, the reaction mixture was extracted using 30 mL of deionized water and 30 mL of DCM in a separatory funnel. The organic layer was collected leaving the less dense aqueous layer in the funnel which was washed twice more with two portions of 30 mL of DCM. The organic layer was collected and dried using anhydrous Na₂SO₄. This product was recovered using rotary evaporation.¹⁸

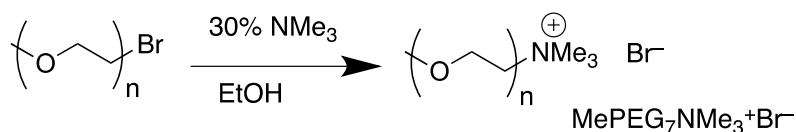


Figure 9: Synthesis of MePEG₇NMe₃⁺ Br⁻ (MW = 472.015 g/mol)

To verify the success of the synthesis, Nuclear Magnetic Resonance (NMR) spectra were obtained for both ^1H , **Figure 10**, and ^{13}C , **Figure 11**. The $\text{MePEG}_7\text{NMe}_3^+ \text{Br}^-$ was analyzed in CDCl_3 for both spectra. In the proton spectrum, there are notable peaks at 1.23 ppm, 2.87 ppm, several clusters in the 3.45-3.81 ppm range, 3.95 ppm, and 5.31 ppm. A peak at 7.30 ppm represents the solvent, CDCl_3 . The peak at 2.87 ppm identifies the NMe_3 group attached to the MePEG_7 molecule which indicates the reaction produced $\text{MePEG}_7\text{NMe}_3^+ \text{Br}^-$. The ^1H NMR of MePEG_7Br indicated the peak at 3.81 ppm correlated with the protons on the methylene group adjacent to the bromide.²¹ In **Figure 10**, it is unclear from the ^1H NMR if any MePEG_7Br remains unreacted in the final solution because the spectrum is highly clustered in this region.

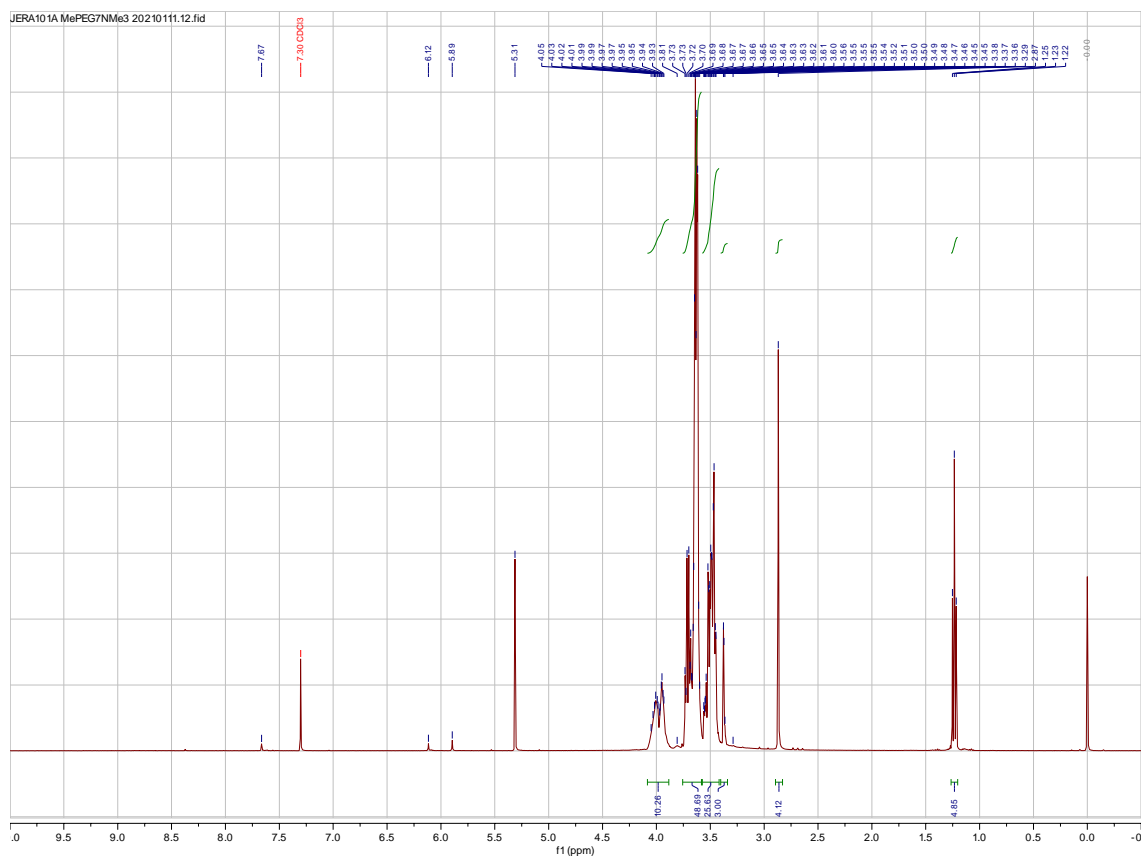


Figure 10: The ^1H NMR for $\text{MePEG}_7\text{NMe}_3^+ \text{Br}^-$

The ^{13}C NMR displays similar patterns to the proton NMR. It has major peaks at 18.44 ppm, 44.99 ppm, 54.58 ppm, 58.20 ppm, 65.29 ppm, and 70.58 ppm. The peaks from 76.77-77.41 ppm represent the CDCl_3 and therefore are excluded from the data. The peak at 18.44 ppm represents the carbons in the NMe_3 group in $\text{MePEG}_7\text{NMe}_3^+ \text{Br}^-$.²⁸ From the previous ^{13}C NMR of MePEG_7Br , the peak at 30.34 ppm represented the carbon attached to the bromide group in MePEG_7Br . The absence of this peak in **Figure 11** indicates that the reaction went to 100% completion.

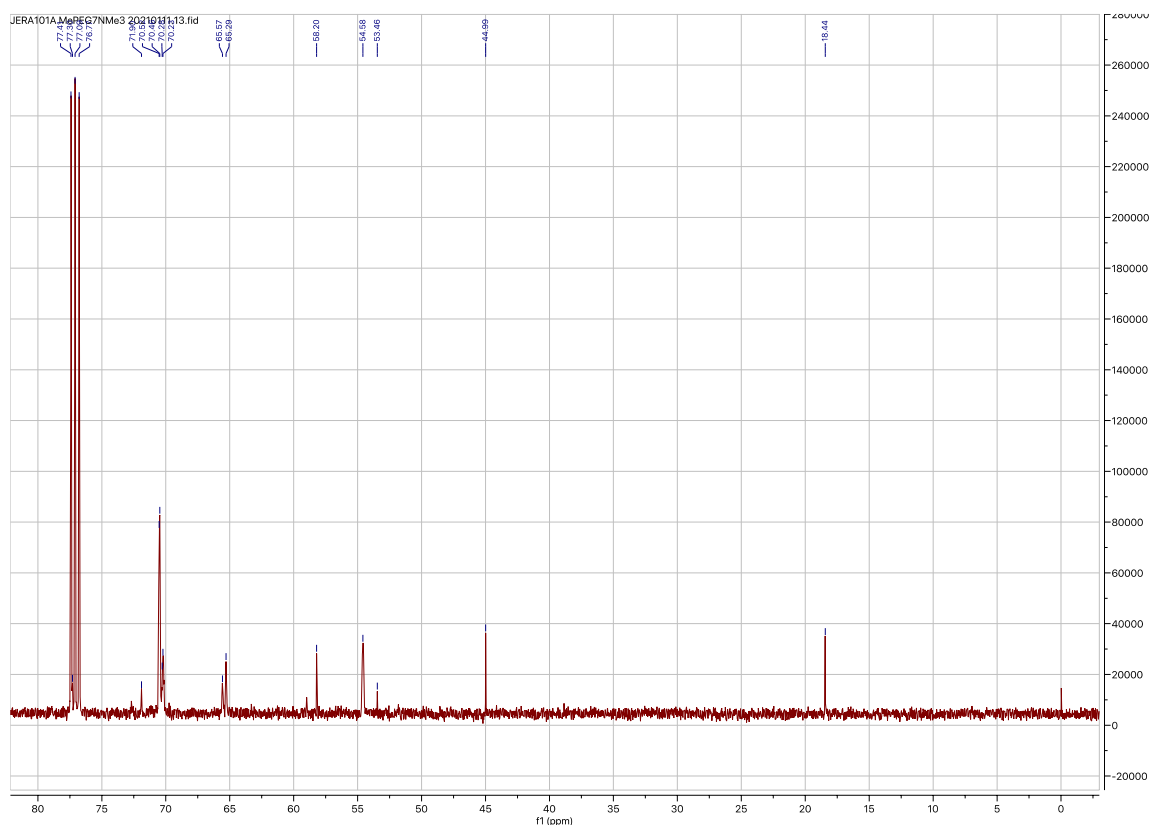


Figure 11: The ^{13}C NMR for $\text{MePEG}_7\text{NMe}_3^+ \text{Br}^-$

Ion Exchange of MePEG₇NMe₃⁺ Br⁻ to MePEG₇NMe₃⁺ OH⁻

To achieve the final product MePEG₇NMe₃⁺ OH⁻, the bromide counter-ion must be exchanged with a hydroxide ion. In order for this reaction to occur, a strongly basic exchange column was used. The anion exchange column was filled with 160 mL of Amberlite IRA-400 chloride-form, a strongly basic ion-exchange resin. The column and resin were then rinsed with nanopore water and then charged using 150 mL of a 4.0 M solution of sodium hydroxide (NaOH, 39.99 g/mol). This will exchange the chloride ions on the resin with hydroxide ions. The column was then rinsed with nanopore water until the pH was around 8.0. A solution of water with MePEG₇NMe₃⁺ Br⁻ was slowly run through the column and rinsed with nanopore water. As the MePEG₇NMe₃⁺ Br⁻ was run through the column, the bromide ions were exchanged with hydroxide ions, and MePEG₇NMe₃⁺ OH⁻ was eluted from the bottom of the column. While MePEG₇NMe₃⁺ OH⁻ was eluting, the pH of the eluent was very basic. The column was rinsed with additional water until the effluent reached a pH of around 8.0. The more neutral eluent indicated that the MePEG₇NMe₃⁺ OH⁻ (MW = 409.11 g/mol) product had been completely eluted through the column. Ethanol was added to the eluent to reduce the boiling point of the solution. The MePEG₇NMe₃⁺ OH⁻ product was recovered using rotary evaporation.¹⁹ The synthesis can be seen in *Figure 12*.

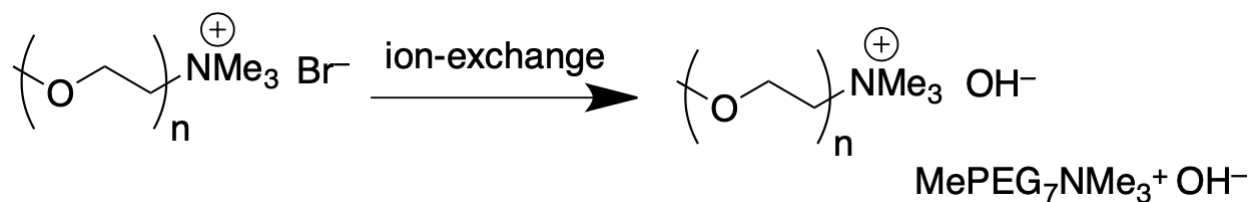


Figure 12: Synthesis of MePEG₇NMe₃⁺ OH⁻ (MW = 409.11 g/mol)

To assay the success of the ion-exchange, a small aqueous sample of the MePEG₇NMe₃⁺ OH⁻ ion-exchange product was titrated with Methane Sulfonic Acid (MeSO₃H) to a pH of 7.00. This should form MePEG₇NMe₃⁺ MeSO₃⁻. The ¹H-NMR was then recorded for this compound, and the areas of the MeSO₃⁻ peak and the CH₃O- and the NMe₃ peaks were compared.

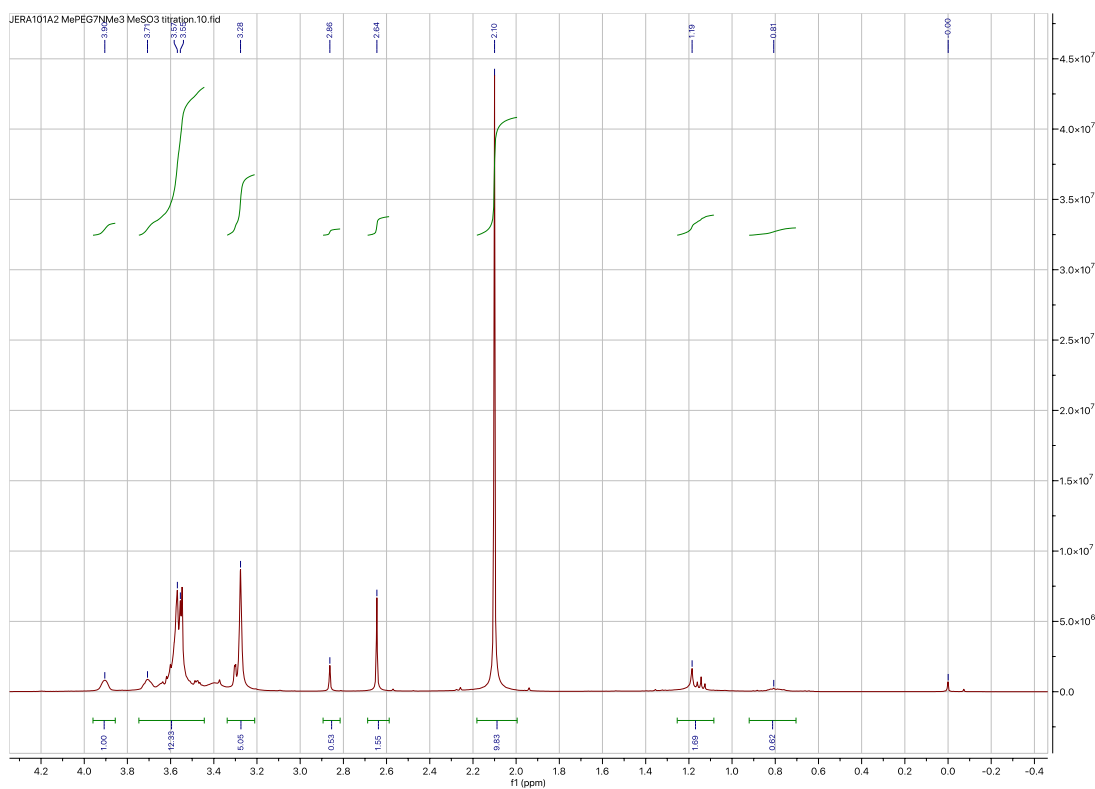


Figure 13: The ¹H NMR for MePEG₇NMe₃⁺ CH₃SO₃⁻

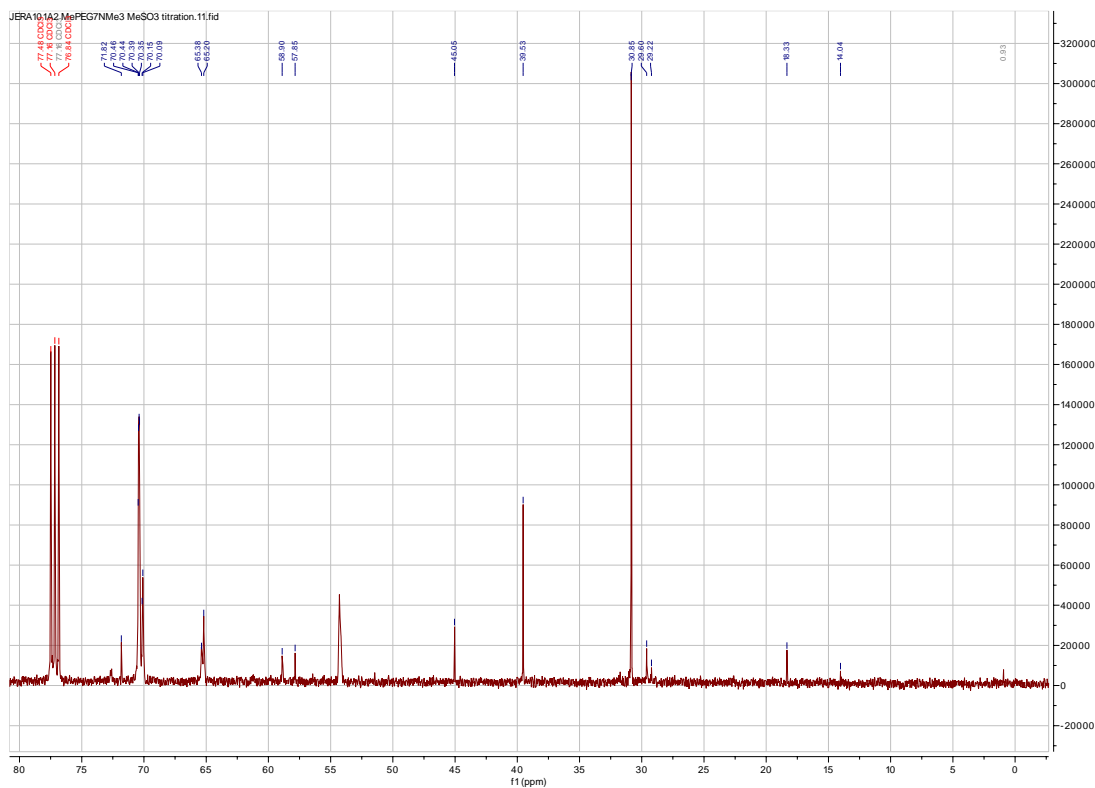


Figure 14: The ^{13}C NMR for $\text{MePEG}_7\text{NMe}_3^+ \text{CH}_3\text{SO}_3^-$

Formation of MePEG₇ Li⁺ Solution

A $\text{MePEG}_7 \text{Li}^+$ solution was prepared using 0.331 g of LiPF_6 (MW = 151.905 g/mol) and 2.0 mL of MePEG_7 (MW = 350 g/mol). This resulting solution had a molarity of 1.0. This solution serves as a guide for accuracy and precision for the AC impedance spectroscopy. While this solution measures the movement of Li^+ ions across the membrane instead of OH^- , it still serves as a guide to analyze the mechanisms of MePEG_7 based polymers.

Conductivity Measurements

The conductivity measurements were performed using a PAR 283 Potentiostat with a Perkin-Elmer 5210 lock-in amplifier, shown in **Figure 15**. These instruments were controlled by the PowerSuite software to change the parameters of the experiments and the software also collected and analyzed the data collected.

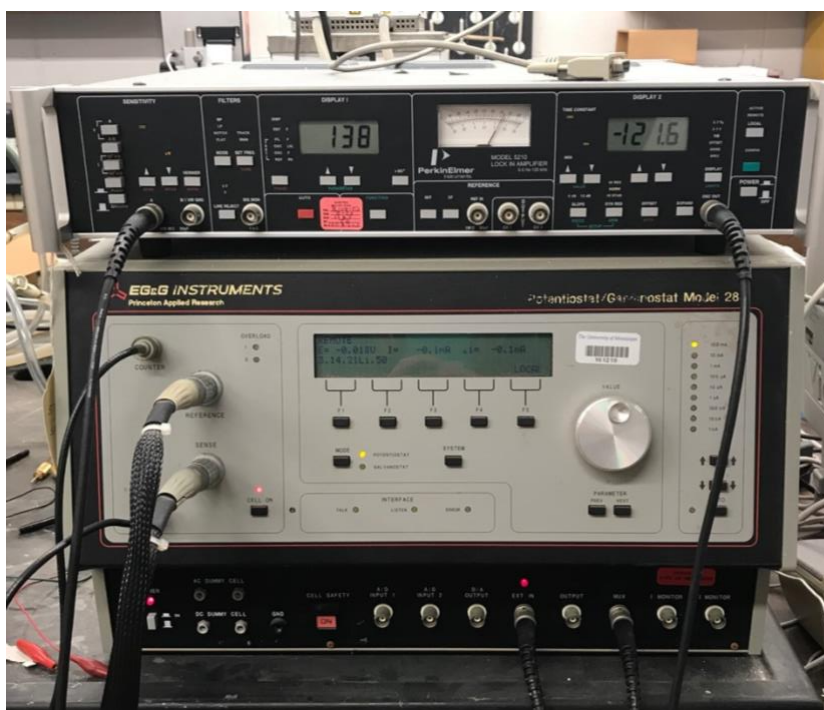


Figure 15: Perkin-Elmer 5210 Lock-in Amplifier (top) and PAR 283 Potentiostat (bottom)

The basic set up for the conductivity measurements are shown in **Figure 16**. A Faraday Cage enclosed the electrode and their connections. We performed the experiments inside the cage because the electrostatic repulsion of charges causes a redistribution of charge to the outside of the conductor. This results in a net electrostatic

field of zero within the conductor.¹⁶ Essentially, the Faraday Cage cancels all electric noise from outside of the cage. Water and vacuum tubing can be seen in **Figure 16** because the experiments were run under a temperature controlled dry condition.

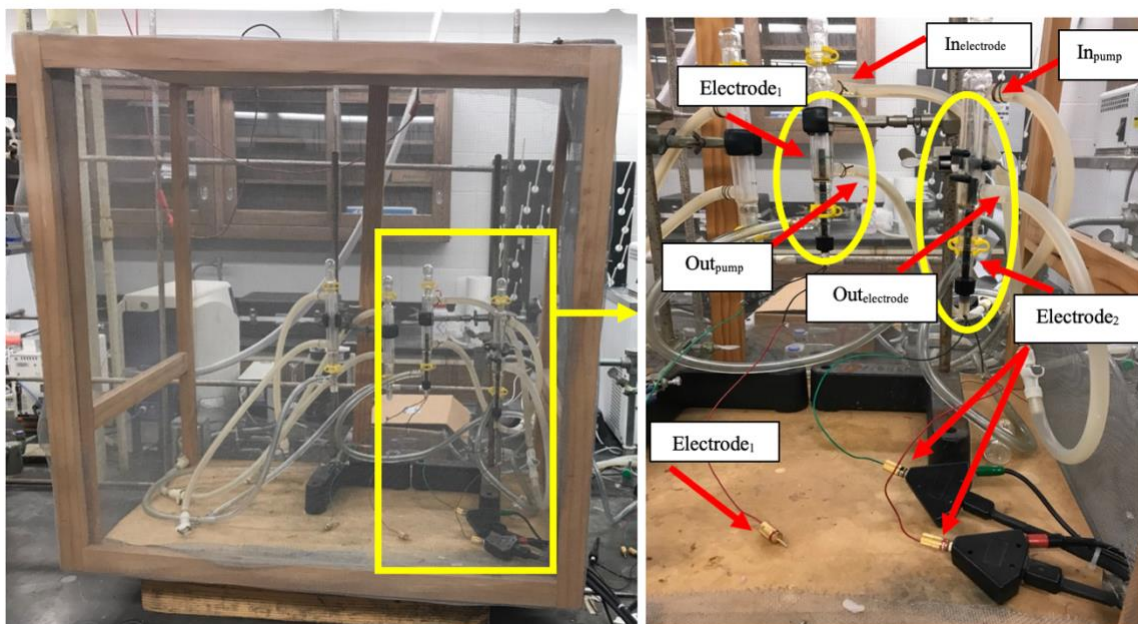


Figure 16: A Faraday Cage (left) Enclosing the Temperature and Vacuum Controlled Electrode System (right)

Dry conditions are necessary because the water in the air can be absorbed by the PEG-based electrolyte, and can dramatically increase the ionic-conductivity values obtained. An Isotemp 3016 water heater and cooler along with a MaximaDry vacuum pump were used to create these conditions, shown in **Figure 17**. The water heater and cooler were connected to one Electrode₂ which was connected to Electrode₁ which pumped the water back to the water heater and cooler. The vacuum was connected the same way. This meant the system could test two electrodes at a time. The connections just needed to be switched when the different polymers were measured.

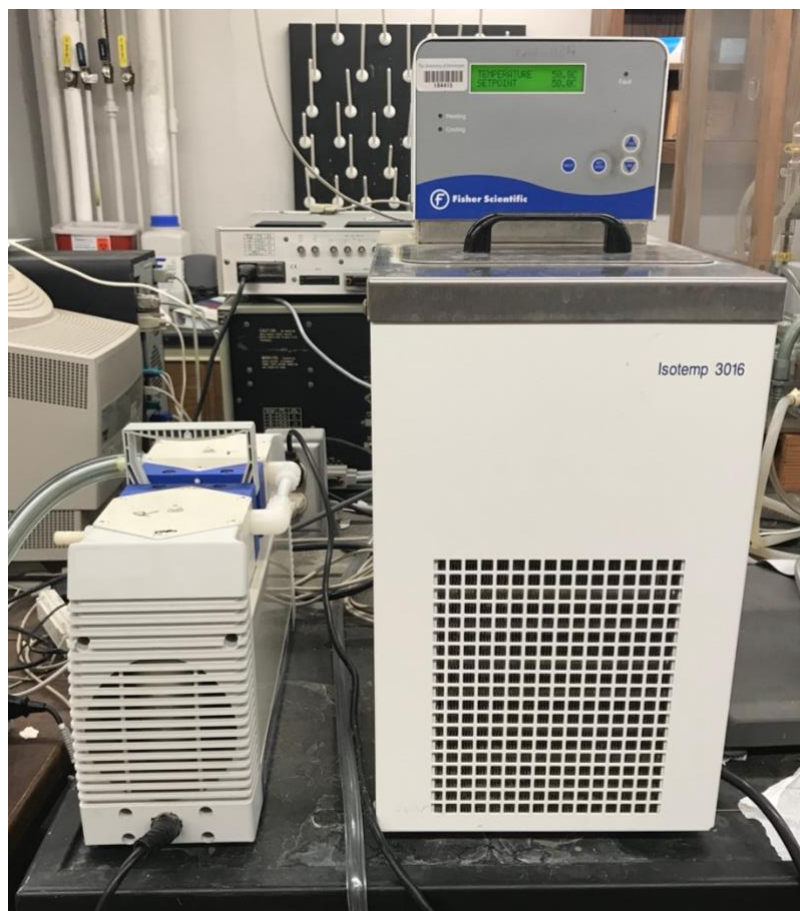


Figure 17: MaximaDry Vacuum Pump (left) and an Isotemp 3016 Water Heater and Cooler (right)

To ensure the instruments and software were calibrated, a “dummy cell” was tested. The AC Impedance Dummy Cell 1700-1126-REV. 0 used is shown in *Figure 18* which had a resistance of $100 \pm 20\% \Omega$. Once the Nyquist Plot for the dummy cell displayed a diameter within the range of $100 \pm 20\% \Omega$, then further experiments could be conducted.

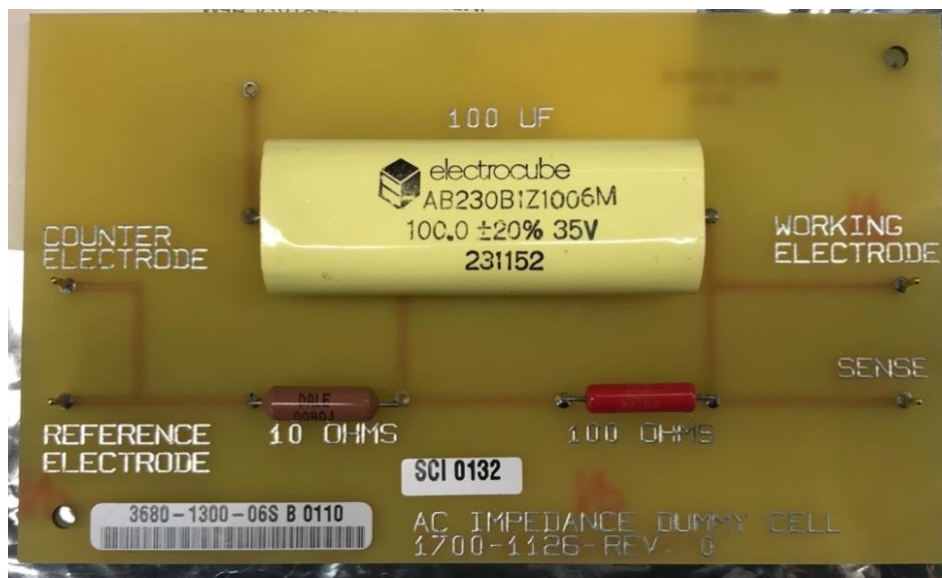


Figure 18: AC Impedance Dummy Cell 1700-1126-REV. 0

Before the conductivity tests of the MePEG₇ Li⁺ solution and MePEG₇ – NMe₃⁺ OH⁻ polymer could be conducted, they had to be dried out. A few drops of the solutions were added to the top of the electrode and gently sealed in the system. Then, the system was heated at 50 °C under vacuum for 2 hours before testing. Measurements were taken from 10-80 °C in increments of 10 °C of each molecule using the parameters shown in *Figure 19*. These temperatures were chosen to be measured because they are similar to the temperatures that the AEMFCs operate at. The Test 22421 corresponds with the dummy cell; 3.6.21Li.20 corresponds to the MePEG 350 Li⁺ solution; and the 3.6.21SMP27A.20 corresponds with the MePEG₇ – NMe₃⁺ OH⁻.

Parameters	Test 22421	3.6.21Li.20	3.6.21SMP27A.20
Start Frequency	3.00 kHz	120 kHz	120 kHz
End Frequency	100 mHz	50.0 Hz	300 Hz
AC Level	10 mV	10.0 mV	10.0 mV
Current Ranging	Fixed 1.00 mA	Automatic (10.0 mA)	Automatic (10.0 mA)
Electrode Area	1.00 cm ²	1.00 cm ²	1.00 cm ²
Calibration Dataset	Old 283 Z Calibration	Old 283 Z Calibration	Old 283 Z Calibration

Figure 19: The Parameters for the Conductivity Measurements in PowerSuite

Once the data was obtained in PowerSuite it was analyzed using the Nyquist Plot and verified using Bode Plots, which measures the resistance versus frequency.⁹ The frequency range was limited to display the semicircle and very few points of the Warburg tail. A best circle fit was selected for each data set to find the diameter. Data points that fell outside of the range that seemed visibly reasonable were excluded. These points show sharp deviations from the normal trend in the Nyquist Plot. In addition, the Bode Plot could be used to verify if the point was abnormal data.⁹ If the data point deviated from both trends in the Nyquist Plot and the Bode Plot it was excluded. Due to the age of the equipment, operating system, and the computer itself, these points occurred frequently. To ensure the precision of the data, the tests were run four times at each data point and then averaged. Once the average diameter of the semicircle was recorded at each temperature point, it could be converted from resistance to conductivity. The conductivity electrode used has a cell constant of 1.0 cm⁻¹ which is needed for the conversion from

conductance to conductivity. Sample calculations can be seen below. The data was then plotted log (conductivity) versus 1000/K to determine the activation energy from the slope.

Sample Calculations to Determine E_a from Nyquist Plot

$$S = 1/\Omega = 1 / 1.26E+06 \Omega = 9.09E-07 \text{ Siemens}$$

$$\sigma = S (l/A) = 9.09E-07 \text{ S} (1/12.1 \text{ cm}) = 7.51E-08 \text{ S/cm}$$

$$\log(\sigma) = \log (7.51E-08 \text{ S/cm}) = -7.15$$

$$1000/ K = 1000/ (10 + 273.15) = 3.53 \text{ 1/K}$$

$$E_a = \text{Slope} * \ln(10) * 8.314 \text{ J/mol}\cdot\text{K} = X \text{ kJ/mol}$$

Molar Conductivity Measurements

To determine the concentration of the sample, the density had to be found. Using a ATI CAHN C-33 Microbalance and a Microliter #703 pipette, 10 μL of the sample were pipetted and then weighed. Due to the high degree of possible error and sensitivity of the instruments, the measurements were repeated three times. The density (g/mL) could be found by dividing the mass by the volume. The concentration of the sample was then calculated using the molar mass of the final product, 409.11 g/mol. Then, the conductivity measurements found in earlier steps were divided by the concentration in such a way to yield a final unit of $\text{S cm}^2 \text{ mol}^{-1}$. Since the LiPF_6 MePEG 350 solution had a known concentration of 1.0 M, the concentration did not need to be found. The density of the solution was measured to compare to the synthesized polymer.

RESULTS AND DISCUSSION

AC Impedance Dummy Cell 1700-1126-REV

The Nyquist Plot for the AC Impedance Dummy Cell with an interfacial resistance of 10Ω and a bulk resistance of $100 \pm 20\% \Omega$ is seen in **Figure 20**. The plot displays a semi-circle with a best circle fit that has a diameter of 99.81Ω within the range of 25.8 - 123.3Ω . The sample deviation for this circle fit is very small, 0.4304 . Based on these observations, it can be concluded that the instrument was properly calibrated because the experimental value fell within the range of resistance, 95 - 105Ω . However, it is important to note that because of the 10Ω of interfacial resistance, the circle should have the range of 10 - 110Ω ; this shows that there is additional, unknown interfacial resistance present, but, this does not appear to affect the bulk resistance because the diameter was well within acceptable parameters.

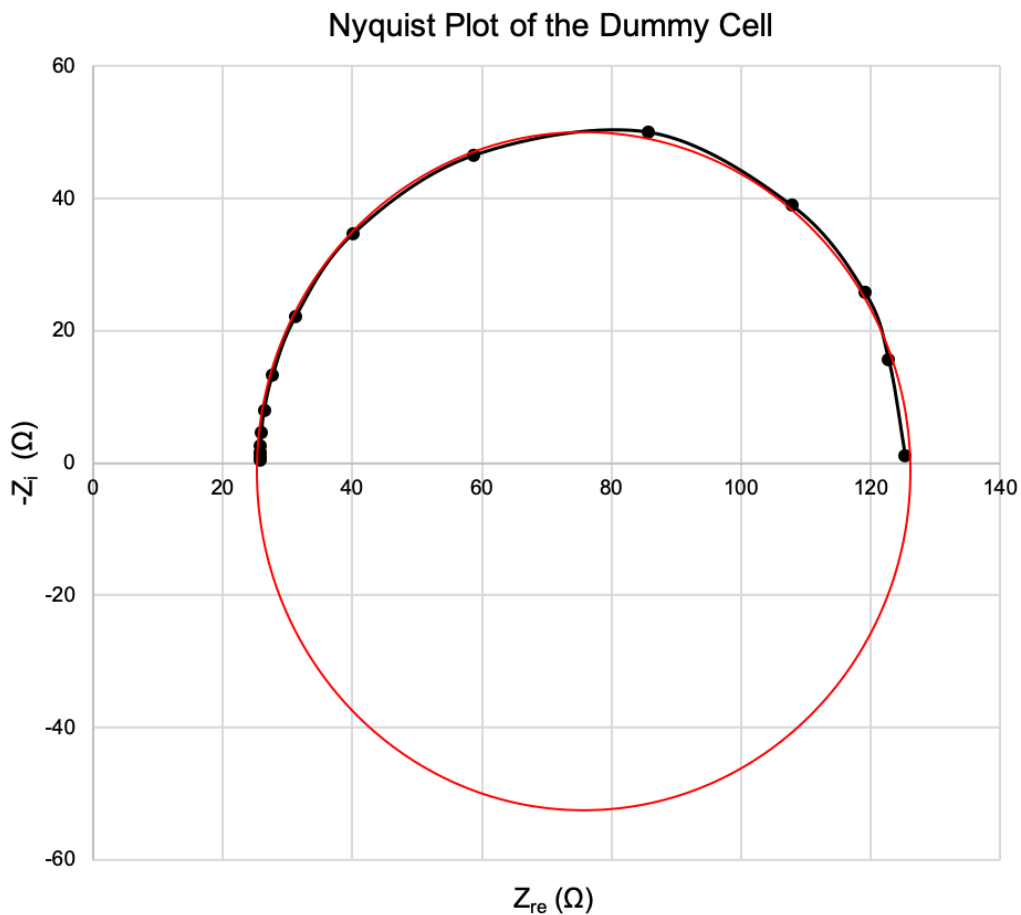


Figure 20: Nyquist Plot for AC Impedance Dummy Cell which had a diameter of 99.81 Ω

Conductivity Results

The temperature dependent resistance values of MePEG₇ Li⁺ and MePEG₇NMe₃⁺ OH⁻ were collected from the best circle fit diameters as shown in **Figure 21** and **Figure 22**. As the temperature increased, the shape of the semicircle degraded slightly. The frequency was selected for each polymer electrolyte to minimize the Warburg tail and maximize the number of points in the semicircle impedance range to preserve the validity of the best circle fit. These figures only display one data point for each polymer, however, a Nyquist Plot was created for each data point and the resistance from the

diameter was collected and converted to conductivity. The conductivity averages for MePEG₇ Li⁺ and MePEG₇NMe₃⁺ OH⁻ were reported in *Figure 23*.

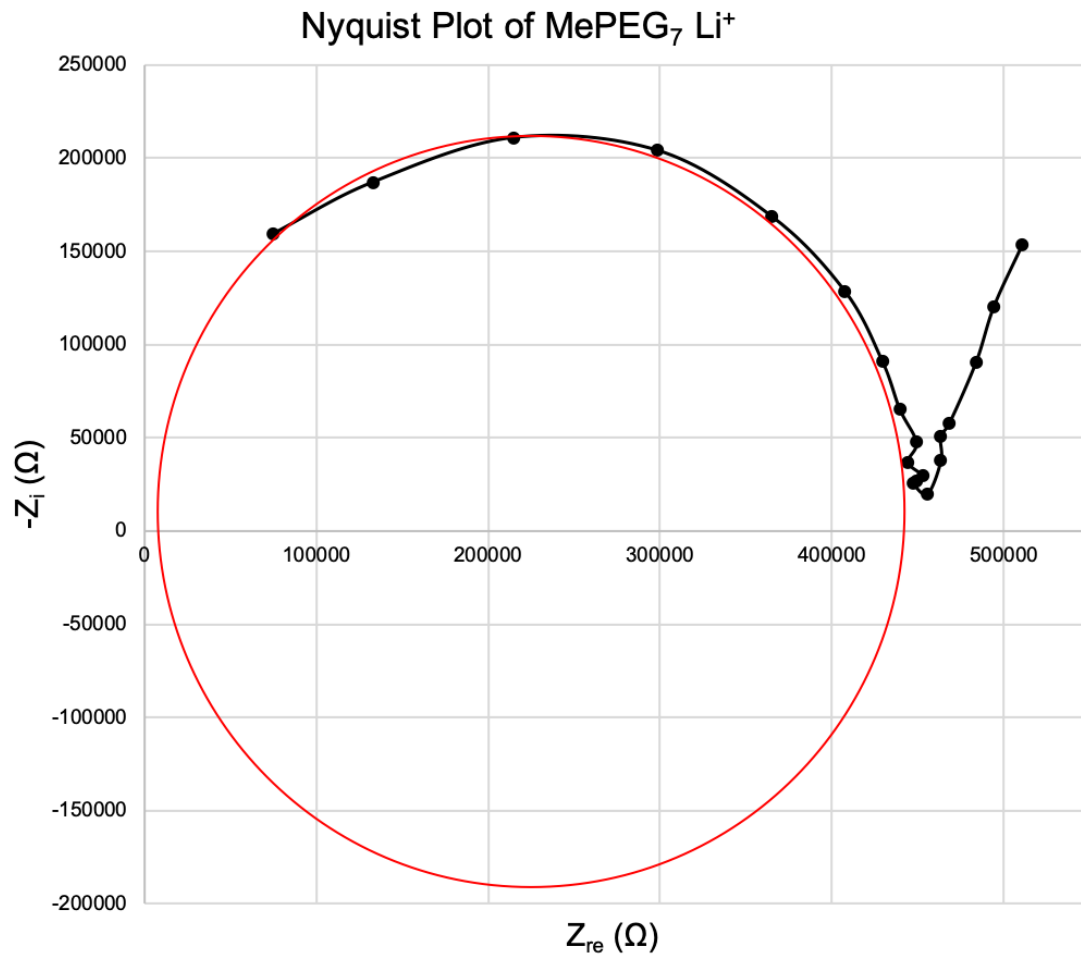


Figure 21: Nyquist Plot of MePEG₇ Li⁺ at 20 °C which had a diameter of 450,400 Ω and conductivity of $2.22 \cdot 10^{-6}$ S/cm

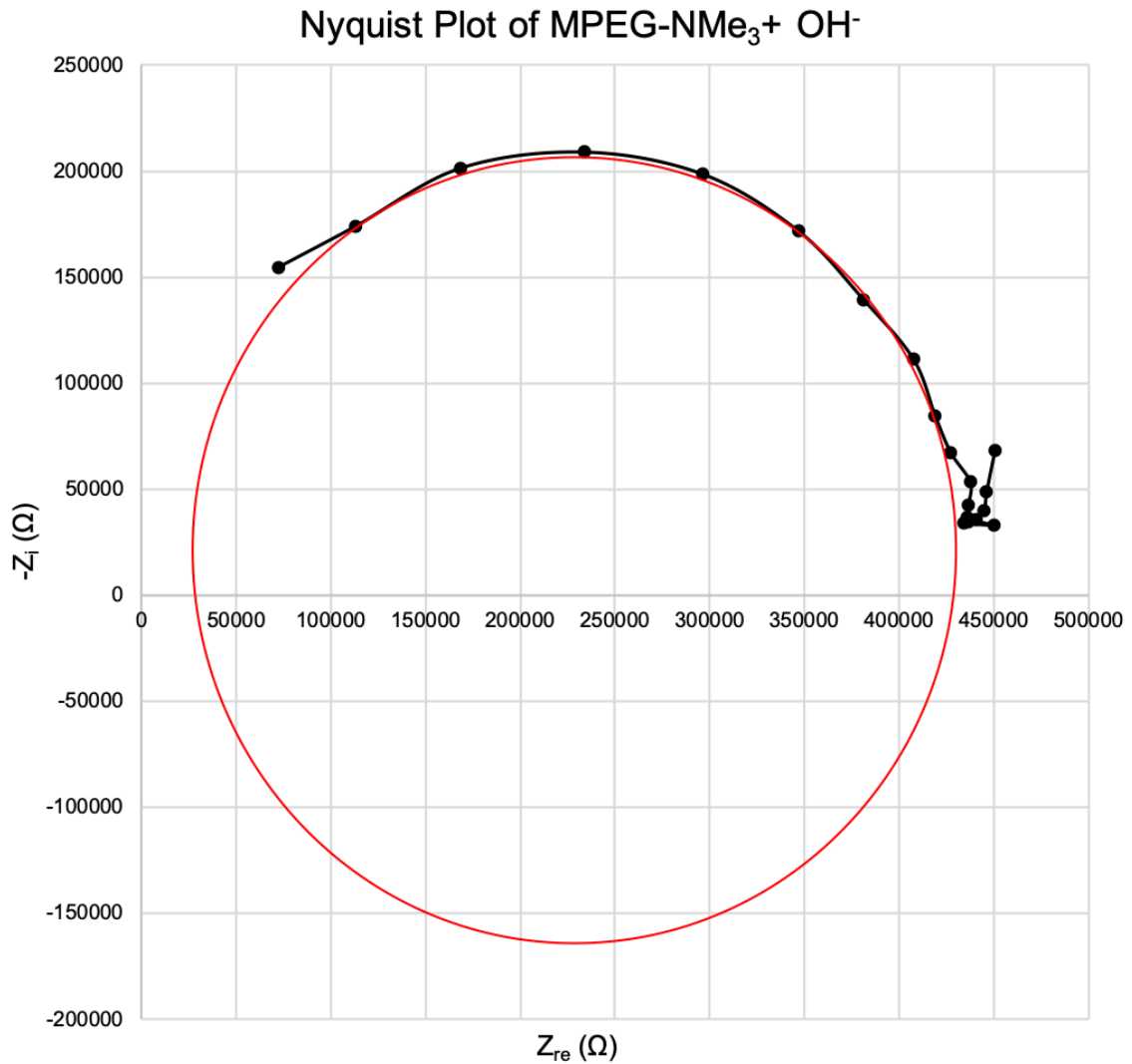


Figure 22: Nyquist Plot of MePEG₇NMe₃⁺ OH⁻ at 20 °C which had a diameter of 433,500 Ω and conductivity of 2.31*10⁻⁶ S/cm

The conductivity of both polymer electrolytes displayed a direct relationship with temperature as shown in **Figure 23**. As the temperature increased, the conductivity did as well which is consistent with the literature. An increase in temperature increases the kinetic energy and velocity of the molecules and atoms in the solution. Since the polymer is immobile in the AEMFCs, they hydroxide ions activity across the membrane will increase, allowing them to pass through the polymer membrane quicker which increases

the conductivity. At a certain temperature point, the conductivity will not increase because the polymer membrane itself will degrade. The kinetic energy of the electrons at this point will be stronger than the energy between the bonds. Polymer electrolytes that have a high temperature resistance are attractive for AEMFCs because it expands the conditions the cell can operate at which is currently limited.¹¹

Temperature (°C)	MePEG ₇ Li ⁺ (μS/cm)	MePEG ₇ NMe ₃ ⁺ OH ⁻ (μS/cm)
10	1.20	0.909
20	1.99	1.66
30	2.91	2.85
40	3.83	4.82
50	10.9	21.5
60	28.2	16.2
70	33.7	26.9
80	23.8	44.7

Figure 23: Temperature dependent conductivity measurements for MePEG₇ Li⁺ and MePEG₇NMe₃⁺ OH⁻

The molar conductivity of the two solutions are displayed in *Figure 24*. The MePEG Li⁺ solution had a higher molar conductivity than the MePEGNMe₃⁺ OH⁻, however, the values at lower temperatures were more similar between the two solutions. The difference between the two polymers may be attributed to the difference in ion used

in this solution or the attachment of the trimethylamine group to MePEG₇ polymer. Despite these two differences between the solutions, the molar conductivities remain relatively similar suggesting that the polymer backbone plays a larger role than ionic groups attached or the ion that is being transported.

Temperature (°C)	MePEG ₇ Li ⁺ (μS cm ² mol ⁻¹)	MePEG ₇ NMe ₃ ⁺ OH ⁻ (μS cm ² mol ⁻¹)
10	1.20	0.338
20	1.99	0.620
30	2.91	1.06
40	3.83	1.79
50	10.9	8.01
60	28.2	6.05
70	33.7	10.0
80	23.8	16.6

Figure 24: Temperature dependent molar conductivity measurements for MePEG₇ Li⁺ and MePEG₇NMe₃⁺ OH⁻. The density of the MePEG₇ Li⁺ solution was found to be 1.23 ± 0.03 g/mL. The density of the MePEG₇NMe₃⁺ OH⁻ 1.10 ± 0.08 g/mL.

The Arrhenius Activation Plot for MePEG₇ Li⁺ shown in **Figure 25** yielded an activation energy of 39.31 kJ/mol. The activation energy describes the amount of energy per mole needed to transport the ion across the membrane. The activation energy and the conductivity of poly (ethylene glycol) methyl ether polymer for lithium ions is consistent

with other polymers in analyzed in the literature.²⁶ Its activation curve typically displays curvature in graph at higher temperatures which is consistent with the data collected. A linear fit was used to analyze the data, however, the Vogel-Fulcher-Tammann (VTF) equation can be used to better describe the relationship.²⁷ Despite this, the coefficient of determination is still high suggesting that the linearity deviates at much higher temperatures. The deviation seen in **Figure 25** could be related to error in instrumentation or failure to completely dry the sample. Both of these deviations would be seen in individual data points which would lower or raise the average of conductivity at the temperature point depending on the deviation.

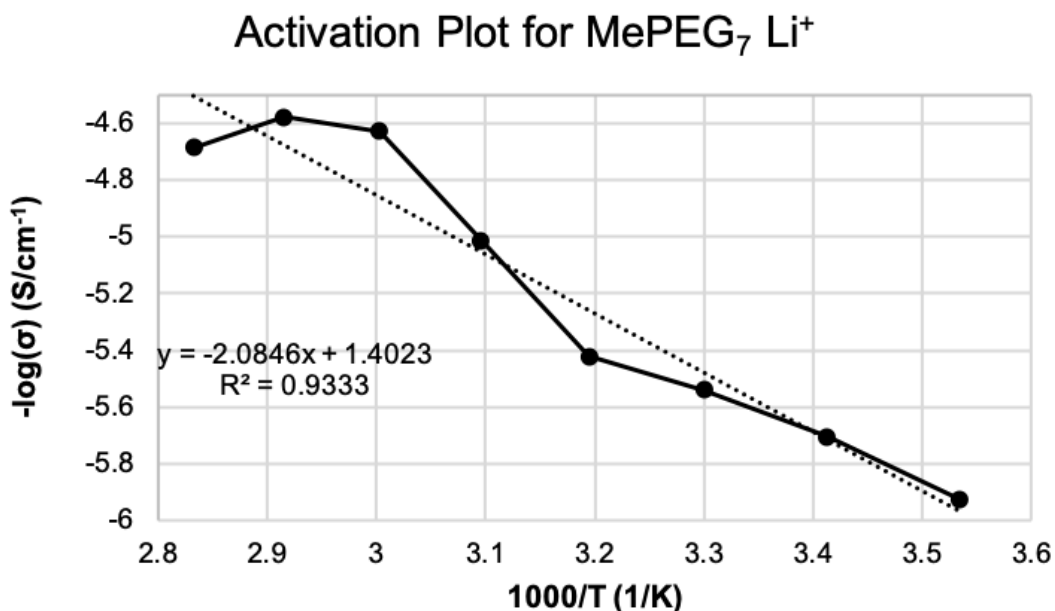


Figure 25: Arrhenius Activation Plot for MePEG₇ Li⁺, best fit line and coefficient of determination displayed. The slope yielded an activation energy of 39.31 kJ/mol.

Despite the MePEG₇ Li⁺ solution transporting lithium ions, analyzing the conductivity with polymer electrolytes that transport other ions, such as hydroxide is useful. Lithium ion transport has been well studied due to its prevalence in batteries. Batteries, like fuel cells, transfer ions across an electrolyte. Lithium ion batteries are one of the most common types of batteries and have undergone extensive research and development. The conductivity measurements of lithium ions are common in the literature, allowing for the precision and accuracy of the AC Impedance Spectroscopy instrumentation and methods to be further determined with a solution that was quickly and easily created. The comparison of the two polymer electrolytes is useful because both contain a MePEG 350 backbone.

The Arrhenius Activation Plot for MePEG₇NMe₃⁺ OH⁻ shown in **Figure 26** yielded an activation energy of 42.24 kJ/mol and a coefficient of determination value, 0.9954, that shows a highly linear relationship between the variables. The activation energies for MePEG₇ Li⁺ and MePEG₇NMe₃⁺ OH⁻ are similar which suggests that two have similar mechanisms for ionic conductivity. The MePEG 350 polymer backbone seems to indicate that the mechanism for ionic conductivity is affected greater by the structure of the polymer rather than the ion being transported. The lithium ion and hydroxide ion are similar in physical size which could also contribute to similar activation energies. The charges on the ions do not seem to affect the activation energy despite one being cationic and the other being anionic. This suggests that polymer electrolytes can be used to transport both anions and cations, and, if true, would be a useful property of these molecules for the development of fuel cells.

The activation energy, 42.24 kJ/mol, of the MePEG₇NMe₃⁺ OH⁻ is consistent with other conductivity studies of other anhydrous hydroxide ion conducting polymer electrolytes tested in this lab group¹⁹. However, the conductivity values are lower than the values in the literature and the activation energy is higher than values in the literature.^{22, 23, 24, 25} Activation energies for hydroxide ion conducting polymers are shown to have a wide range of values, however, some are known to be near 10-15 kJ/mol.²⁵ The value obtained in this experiment fall in the range of energies, however, they are significantly higher than those in the low range. Lower activation energies are ideal because it could potentially allow for different catalysts or fuels to be used, thus, MePEG₇NMe₃⁺ OH⁻ is not a good alternative to polymers used in AEMFCs in this sense. The conductivity values, typically around 10-1000 μS/cm depending on the temperature, follow a similar pattern, except, higher conductivity values are ideal because the ions are transported across the membrane more efficiently allowing for improved fuel cell performance. The conductivity values of MePEG₇NMe₃⁺ OH⁻, 0.9-44.7 μS/cm, suggest that it is not an ideal replacement for AEMFCs if the goal was to improve ionic conductivity.

The best fit line on the Arrhenius plot is unexpectedly linear especially at higher temperatures. In this lab group specifically, a deviation from linearity occurs at the higher temperatures suggesting that the electrolyte polymer degrades in some way to prevent it from performing at higher temperatures. However, since the line did not deviate at the higher temperatures, it suggests that MePEG₇NMe₃⁺ OH⁻, may have the potential to still be able to conduct hydroxide ions at high temperatures. This would allow for increased

conductivity and the potential to conduct at temperatures where water is absent from the membrane.

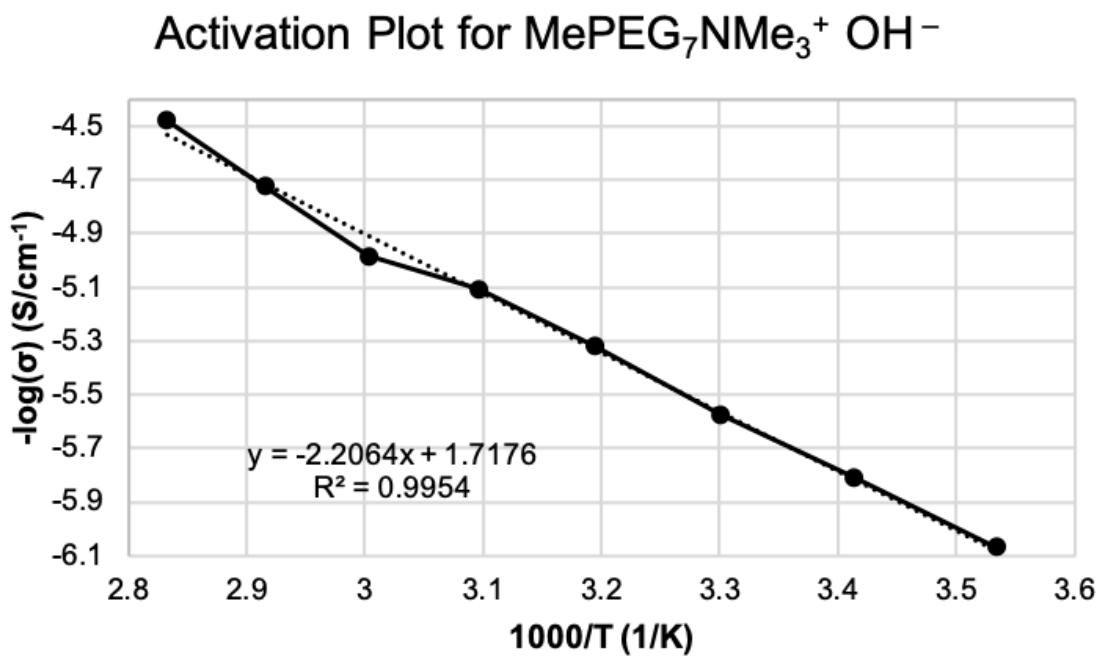


Figure 26: Arrhenius Activation Plot for MePEG₇NMe₃⁺ OH⁻, best fit line and coefficient of determination displayed. The slope yielded an activation energy of 42.24 kJ/mol.

CONCLUSION

In this thesis, a MePEG-based hydroxide, MePEG₇NMe₃⁺ OH⁻, conducting polymer electrolyte was synthesized in order to study the ionic conductivity and its relation to temperature. The backbone of the synthesized polymer, MePEG 350, was also analyzed using ionic conductivity and its relation to temperature, however, a different ion, lithium, was used to measure conductivity. The comparison of MePEG₇ Li⁺ and MePEG₇NMe₃⁺ OH⁻ yielded unexpected similarity in the values of both ionic conductivity, 1.20 - 23.8 μS/cm and 0.91 – 44.7 μS/cm, respectively, and activation energy, 39.31 kJ/mol and 42.24 kJ/mol, respectively, suggestive in similar mechanisms of ion transport. In addition, it suggests that the MePEG₇NMe₃⁺ polymer can be used for both anion and proton exchange membranes because it can transport anions and cations with similar activation energies and conductivities across its membrane. This would be a useful property to further investigate.

The activation energy and ionic conductivity values of MePEG₇NMe₃⁺ OH⁻ are less efficient than polymers reported in the literature. However, the values are consistent with other hydroxide and proton ion conducting polymer electrolytes synthesized in this lab group. The MePEG backbone and the NMe₃ cationic group attached may not be the most effective structures for conductivity purposes. However, this is not the only parameter considered when choosing a polymer electrolyte for an Anion Exchange Membrane Fuel Cell. Parameters within the broad categories of durability, processability, synthesis, and membrane resistance are of similar importance to ionic conductivity.

Therefore, this molecule should be tested and analyzed further to determine its worth as an anion exchange membrane.

While our lab group is interested in improving the ionic conductivity of ion transporting polymers used in fuel cell membranes, we're also very interested in studying and understanding the mechanism of the ion transport through the polymer electrolyte. A great significance is placed on understand the exact movements of the ions as they travel through polymeric electrolytes and is a goal of this lab to determine the similarities between the activation energies of the lithium ion transport and hydroxide ion transport indicate a potential linkage between the mechanisms. We hypothesize that the MePEG may be forming a pseudo crown ether structure where the lithium ions interact in the center; we also hypothesize that the hydroxide ions may be interacting with hydrogen in this structure. This relationship should be further explored and can offer insight to potential mechanisms of ion transport.

The synthesis of polymeric electrolytes is also important to the development of the field. This lab group is one of the few groups that uses new techniques to synthesize polymers ideal for ion exchange membrane fuel cells. In this synthesis, the trimethylamine is a difficult compound to use because at room temperature, this molecule exists as a gas. If the trimethylamine exists in the gas state during the reaction, then the desired product cannot be formed. The hydroxide group on the MePEG is also a very bad "leaving group" and there are very few mechanisms that allow for substitution reactions. This synthesis uses PBr_3 to substitute the hydroxide group with a halide group which is an excellent leaving group. Using techniques to improve the plausibility of difficult steps

is very important to the research of this group. This synthesis process is no different as its execution further develops the field of polymer chemistry.

The research and development of ion exchange membranes is crucial for the future of fuel cells. Fuel cells are becoming an increasingly important, alternative, clean, and renewable energy source. Technical targets, set by the Department of Energy, serve as a guideline for specific areas that need to improve in the development of these fuel cells and membranes.¹⁴ Projects like this are important for the future of clean energy.

REFERENCES

- ¹ O'hayre, R., Cha, S. W., Colella, W., & Prinz, F. B. (2016). *Fuel Cell Fundamentals*. John Wiley & Sons.
- ² Larminie, J., Dicks, A., & McDonald, M. S. (2003). *Fuel Cell Systems Explained* (Vol. 2, pp. 207-225). Chichester, UK: J. Wiley.
- ³ FCHEA. (n.d.). *Fuel Cell Basics*. Retrieved March 20, 2021, from <https://www.fchea.org/fuelcells>
- ⁴ Office of Energy Efficiency and Renewable Energy. (n.d.). *5 Fast Facts About Hydrogen and Fuel Cells*. Retrieved March 20, 2021, from <https://www.energy.gov/eere/articles/5-fast-facts-about-hydrogen-and-fuel-cells>
- ⁵ Office of Energy Efficiency and Renewable Energy. (n.d.). *Fuel Cells*. Retrieved March 20, 2021, from <https://www.energy.gov/eere/fuelcells/fuel-cells>
- ⁶ Tsai, L. D., Chien, H. C., Wang, C. H., Lai, C. M., Lin, J. N., Zhu, C. Y., & Chang, F. C. (2013). Poly (ethylene glycol) Modified Activated Carbon for High Performance Proton Exchange Membrane Fuel Cells. *International Journal of Hydrogen Energy*, 38(26), 11331-11339.
- ⁷ Davydova, E. S., Mukerjee, S., Jaouen, F., & Dekel, D. R. (2018). Electrocatalysts for Hydrogen Oxidation Reaction in Alkaline Electrolytes. *ACS Catalysis*, 8(7), 6665-6690.
- ⁸ EPA. (2019, May 13). *What is CHP?* Retrieved March 20, 2021, from <https://www.epa.gov/chp/what-chp>
- ⁹ GAMRY Instruments. (n.d.). *Basics of Electrochemical Impedance Spectroscopy*. Retrieved March 20, 2021, from <https://www.gamry.com/application-notes/EIS/basics-of-electrochemical-impedance-spectroscopy/>
- ¹⁰ Mei, B. A., Munteshari, O., Lau, J., Dunn, B., & Pilon, L. (2018). Physical interpretations of Nyquist plots for EDLC electrodes and devices. *The Journal of Physical Chemistry C*, 122(1), 194-206.

- ¹¹ Arges, C. G., Ramani, V. K., & Pintauro, P. N. (2010). The chalkboard: Anion exchange membrane fuel cells. *The Electrochemical Society Interface*, 19(2), 31.
- ¹² Harris, J. M. (1985). Laboratory synthesis of polyethylene glycol derivatives. *Journal of Macromolecular Science-Reviews in Macromolecular Chemistry and Physics*, 25(3), 325-373.
- ¹³ Poly(ethylene glycol) METHYL ETHER 81323. (n.d.). Retrieved March 20, 2021, from <https://www.sigmaaldrich.com/catalog/product/aldrich/81323?lang=en&ion=US>
- ¹⁴ Office of Energy Efficiency and Renewable Energy. (n.d.). DOE technical targets for POLYMER Electrolyte membrane fuel cell components. Retrieved March 20, 2021, from <https://www.energy.gov/eere/fuelcells/doe-technical-targets-polymer-electrolyte-membrane-fuel-cell-components>
- ¹⁵ Ramírez, S., & Paz, R. (2018, November 05). Hydroxide transport in ANION-EXCHANGE membranes for alkaline fuel cells. Retrieved March 20, 2021, from <https://www.intechopen.com/books/new-trends-in-ion-exchange-studies/hydroxide-transport-in-anion-exchange-membranes-for-alkaline-fuel-cells>
- ¹⁶ GAMRY Instruments. (n.d.). Faraday Cage: What is It? How does it work? Retrieved March 20, 2021, from <https://www.gamry.com/application-notes/instrumentation/faraday-cage/>
- ¹⁷ Ghosh, B. D., & Ritchie, J. E. (2010). Effect of polymer structure on ion transport in an anhydrous proton conducting electrolyte. *Chemistry of Materials*, 22(4), 1483-1491.
- ¹⁸ Ladner, Andrew, "The Synthesis of a MePEG-based Hydroxide Conducting Electrolyte and the Optimization of the MePEG-Tosylation Reaction" (2020). Honors Theses. 1382. https://egrove.olemiss.edu/hon_thesis/1382
- ¹⁹ Heydinger, Stanton, "A Synthesis and Analysis of Anhydrous Hydroxide Ion Conducting Polymer Electrolytes" (2019). Honors Theses. 1558. https://egrove.olemiss.edu/hon_thesis/1558
- ²⁰ Noh, S., Jeon, J. Y., Adhikari, S., Kim, Y. S., & Bae, C. (2019). Molecular engineering of hydroxide conducting polymers for anion exchange membranes in electrochemical energy conversion technology. *Accounts of chemical research*, 52(9), 2745-2755.
- ²¹ Starkey, L. S. (n.d.). 1H NMR Chemical Shifts. Retrieved March 26, 2021, from <https://www.cpp.edu/~lsstarkey/courses/NMR/NMRshifts1H-general.pdf>

- ²² Thomas, O. D., Soo, K. J., Peckham, T. J., Kulkarni, M. P., & Holdcroft, S. (2012). A stable hydroxide-conducting polymer. *Journal of the American Chemical Society*, 134(26), 10753-10756.
- ²³ Li, J., Qiao, J., & Lian, K. (2020). Hydroxide ion conducting polymer electrolytes and their applications in solid supercapacitors: a review. *Energy Storage Materials*, 24, 6-21.
- ²⁴ Li, J., & Lian, K. (2018). The effect of SiO₂ additives on solid hydroxide ion-conducting polymer electrolytes: A raman microscopy study. *Physical Chemistry Chemical Physics: PCCP*, 20(10), 7148-7155. <https://doi.org/10.1039/C8CP00262B>
- ²⁵ Li, J., & Lian, K. (2018). Investigation of hydroxide ion-conduction in solid polymer electrolytes via electrochemical impedance spectroscopy. *Electrochimica Acta*, 288, 1-11.
- ²⁶ Li, L., Ma, Y., Wang, W., Xu, Y., You, J., & Zhang, Y. (2016). A thermal and electrochemical properties research on gel polymer electrolyte membrane of lithium ion battery. *Journal of Physics and Chemistry of Solids*, 99, 159-166.
- ²⁷ Diederichsen, K. M., Buss, H. G., & McCloskey, B. D. (2017). The compensation effect in the Vogel–Tammann–Fulcher (VTF) equation for polymer-based electrolytes. *Macromolecules*, 50(10), 3831-3840.
- ²⁸ Clark, J. (2020, August 15). Interpreting C-13 NMR Spectra. Retrieved March 26, 2021, from [https://chem.libretexts.org/Bookshelves/Physical_and_Theoretical_Chemistry_Textbook_Maps/Supplemental_Modules_\(Physical_and_Theoretical_Chemistry\)/Spectroscopy/Magnetic_Resonance_Spectroscopies/Nuclear_Magnetic_Resonance/NMR%3A_Experimental/Carbon-13_NMR/Interpreting_C-13_NMR_Spectra](https://chem.libretexts.org/Bookshelves/Physical_and_Theoretical_Chemistry_Textbook_Maps/Supplemental_Modules_(Physical_and_Theoretical_Chemistry)/Spectroscopy/Magnetic_Resonance_Spectroscopies/Nuclear_Magnetic_Resonance/NMR%3A_Experimental/Carbon-13_NMR/Interpreting_C-13_NMR_Spectra)

